Primordial magnetic fields: origin, evolution, and GWs from the early Universe

Invisibles25 (Sep. 2, 2025, CERN)

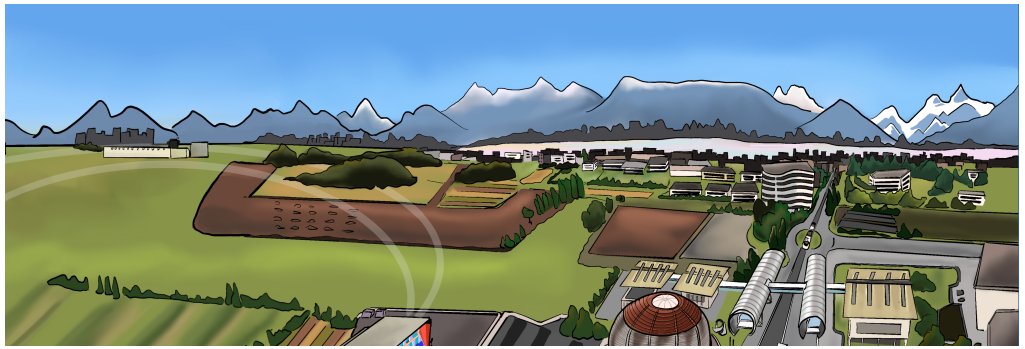

Alberto Roper Pol
University of Geneva

SNSF Ambizione grant (2023–2026): "*Exploring the early universe with gravitational waves and primordial magnetic fields.*"

Collaborators: A. Brandenburg (Nordita), C. Caprini (CERN), T. Kahniashvili (CMU), A. Kosowsky (PittU), S. Mandal (SBU), A. Neronov (APC), D. Semikoz (APC)

Our magnetized Universe

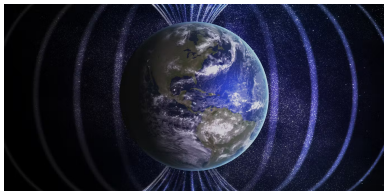

$\sim 1\,\mathrm{G}$

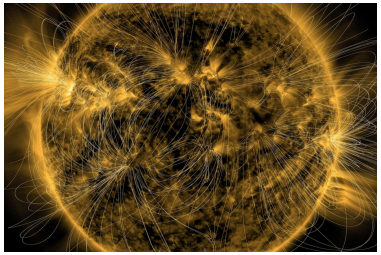

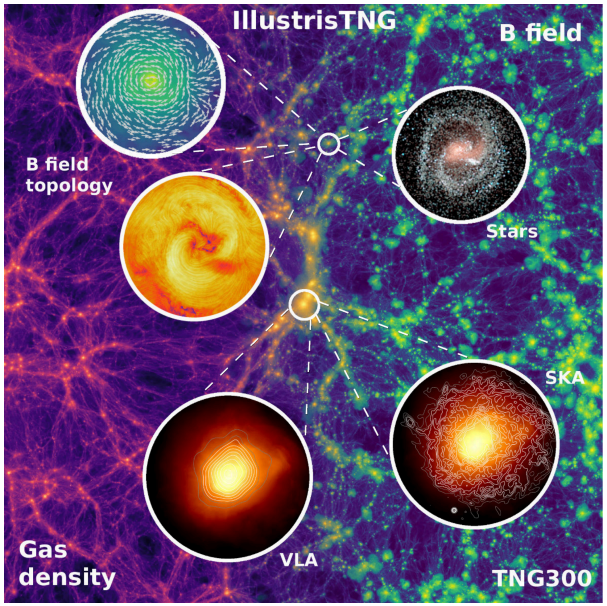

Marinacci et al. (2017), Illustris TNG

$\sim 10^{-9} - 10^{-6}\,\mathrm{G}$

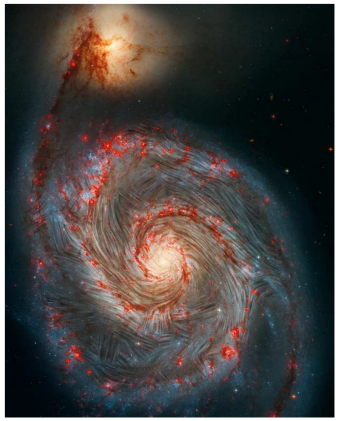

(FIR 145 μm)

(Radio 6 cm Fletcher et. al)

$\sim 10^{-5}\,\mathrm{G}$

Borlaff et al. (2021), SOFIA, M51

- Dense regions in our Universe are strongly magnetized with $B \sim 10\mu$G in galaxies and clusters ($\sim$10 kpc). Radio and far-infrared (FIR) observations.
- Filaments also contain magnetic fields with $B \sim$10 nG (LOFAR observations of Faraday rotation measurements).

Intergalactic magnetic fields in voids of the LSS

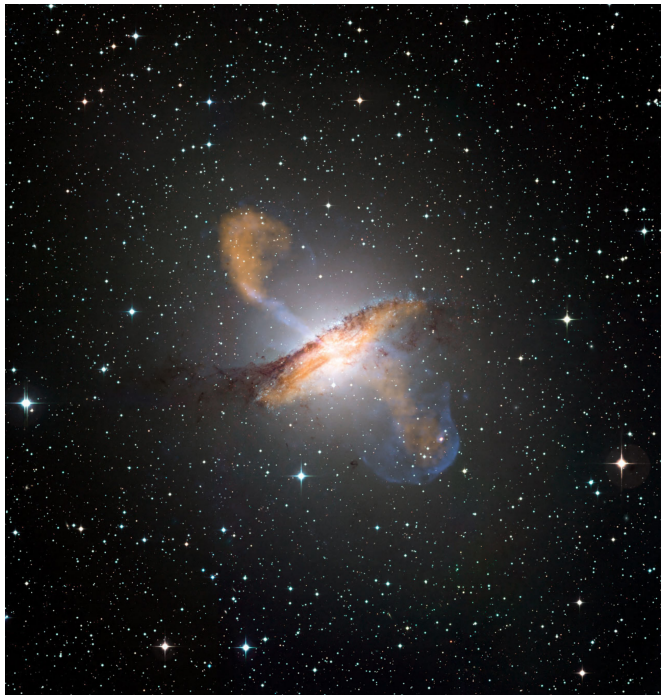

- γ-ray observations from distant blazars by Fermi/MAGIC collaboration show a removal of power at GeV, providing evidence for an intergalactic magnetic field.
- Lower bound of $B \sim 10^{-16}$ G at Mpc scales.

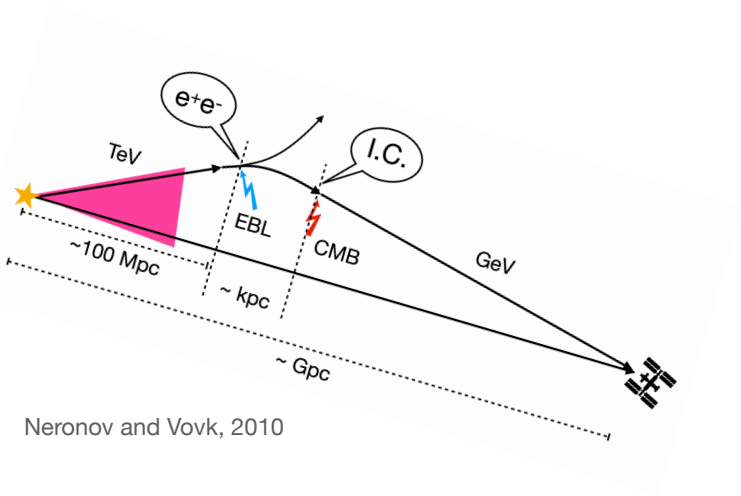

Neronov and Vovk, 2010

Relics from the early Universe?

- The observed intergalactic magnetic fields could have a **primordial** (from inflation or from a phase transition) or an **astrophysical** origin.
- Observations indicate a large volume filling factor in the voids and large correlation length scales (Mpc), favoring a primordial origin.
- Alternative possibilities to explain the blazar observations are:
  - *Beam-plasma instabilities* (suppressing the GeV emission) proposed[1], but seems to not be significant at the intergalactic scales.
  - *Magnetized galactic outflows.* Studied using cosmological simulations. However, it is difficult to reach large volume filling factors.[2]
  - Contribution from *galactic dipoles*,[3] seems plausible but further studies are required.
- Primordial magnetic field present at recombination could alleviate the Hubble tension by reducing the sound horizon.[4]

---

[1] Broderick et al. (2018).
[2] Ni et al. (2024), Tjemsland et al. (2024).
[3] Garg, Durrer & Schober (2025).
[4] Jedamzik & Pogosian (2020).

Generation of primordial magnetic fields

- Magnetic fields could be amplified from quantum fluctuations during inflation or during cosmological phase transitions.
- For inflationary magnetogenesis to be viable, conformal invariance needs to be broken,[5] with $\mathcal{L} \sim f(\phi) F_{\mu\nu} F^{\mu\nu}$ or $g(\phi) F_{\mu\nu} \tilde{F}^{\mu\nu}$. Otherwise, magnetic field perturbations would decay with expansion.
- After reheating, magnetic fields are strongly coupled to the primordial plasma and effectively produce vortical motion, inevitably leading to the development of MHD turbulence.[6]
- Alternatively, small seed magnetic fields can be amplified by primordial turbulence induced by phase transitions, e.g., via dynamo.[7]

---

[5] Turner & Widrow (1988), Ratra (1992), Gasperini *et al.* (1995).

[6] J. Ahonen and K. Enqvist, *Phys. Lett. B* **382**, 40 (1996).

[7] A. Brandenburg *et al.* (incl. ARP), *Phys. Rev. Fluids* **4**, 024608 (2019).

Generation of primordial magnetic fields

- Parity-violating processes during the electroweak phase transition ($T \sim 100$ GeV) are predicted by SM extensions that account for baryogenesis and can produce helical magnetic fields through sphaleron decay or B+L anomalies.[8]

$$\boldsymbol{B} = \boldsymbol{\nabla} \times \boldsymbol{A} - i\frac{2\sin\theta_w}{gv^2}\boldsymbol{\nabla}\Phi^\dagger \times \boldsymbol{\nabla}\Phi$$

- Also after inflation, axion fields can amplify and produce magnetic fields.[9] For example, the QCD axion could oscillate and produce magnetic fields around the QCD scale ($T \sim 100$ MeV).[10]

$$\mathcal{L} \supset \frac{\phi}{f} F_{\mu\nu}\tilde{F}^{\mu\nu}$$

[8] T. Vachaspati, *Phys. Rev. B* **265**, 258 (1991), T. Vachaspati, *Phys. Rev. Lett.* **87**, 251302 (2001), J. M. Cornwall, *Phys. Rev. D* **56**, 6146 (1997).

[9] M. M. Forbes and A. R. Zhitnitsky, *Phys. Rev. Lett.* **85**, 5268 (2000).

[10] Miniati, Gregori, Reville & Sarkar (2018).

Generation of primordial magnetic fields

- Inhomogeneities in the Higgs field in low-scale electroweak hybrid inflation.[11]
- Magnetic fields from inflation can be present and amplified during phase transitions (non-helical[12] and helical[13]).
- Chiral magnetic effect.[14]

[11] M. Joyce and M. E. Shaposhnikov, *Phys. Rev. Lett.* **79**, 1193 (1997), J. García-Bellido *et al.*, *Phys. Rev. D* **60**, 123504 (1999).

[12] M. S. Turner and L. M. Widrow, *Phys. Rev. D* **37**, 2743 (1988).

[13] M. Giovannini, *Phys. Rev. D* **58**, 124027 (1998).

[14] M. Joyce and M. E. Shaposhnikov, *PRL* **79**, 1193 (1997).

GWs from the early Universe

- Gravity is the *weakest fundamental force*. Hence, GWs are difficult to detect but they propagate freely carrying *clean information of the source.*
- Primordial magnetic fields and MHD turbulence in the primordial plasma can produce *a gravitational wave background* potentially observable with *LISA, PTA, or other GW experiments*.
- Observations of gravitational wave backgrounds and primordial magnetic fields can be combined for *multi-messenger studies of the primordial Universe.*
- GWs from the early Universe have the potential to provide us with *direct information on early universe physics* that is *not accessible via electromagnetic observations, complementary to collider experiments*.

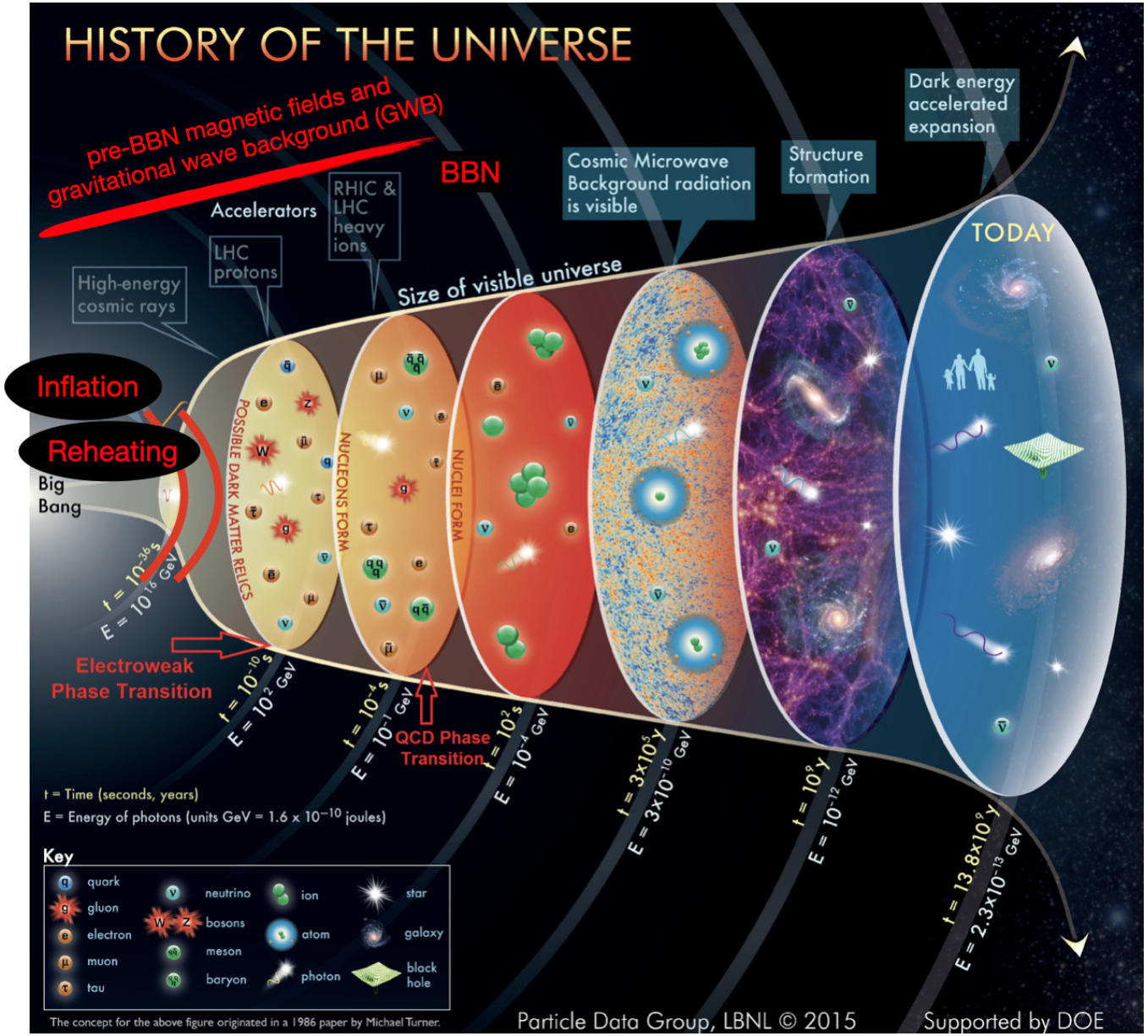
HISTORY OF THE UNIVERSE
pre-BBN magnetic fields and gravitational wave background (GWB)
BBN
Accelerators
RHIC & LHC heavy ions
LHC protons
High-energy cosmic rays
Cosmic Microwave Background radiation is visible
Structure formation
Dark energy accelerated expansion
TODAY
Size of visible universe
Inflation
Reheating
Big Bang
POSSIBLE DARK MATTER RELICS
NUCLEONS FORM
NUCLEI FORM
Electroweak Phase Transition
QCD Phase Transition
t = Time (seconds, years)
E = Energy of photons (units GeV = 1.6 x 10−10 joules)
Key
quark
gluon
electron
muon
tau
neutrino
bosons
meson
baryon
ion
atom
photon
star
galaxy
black hole
The concept for the above figure originated in a 1986 paper by Michael Turner.
Particle Data Group, LBNL © 2015
Supported by DOE

First detections of gravitational waves

- Gravitational waves are opening a new window into our understanding of the Universe
  - First event GW150914 detected by LIGO-Virgo collaboration[15]

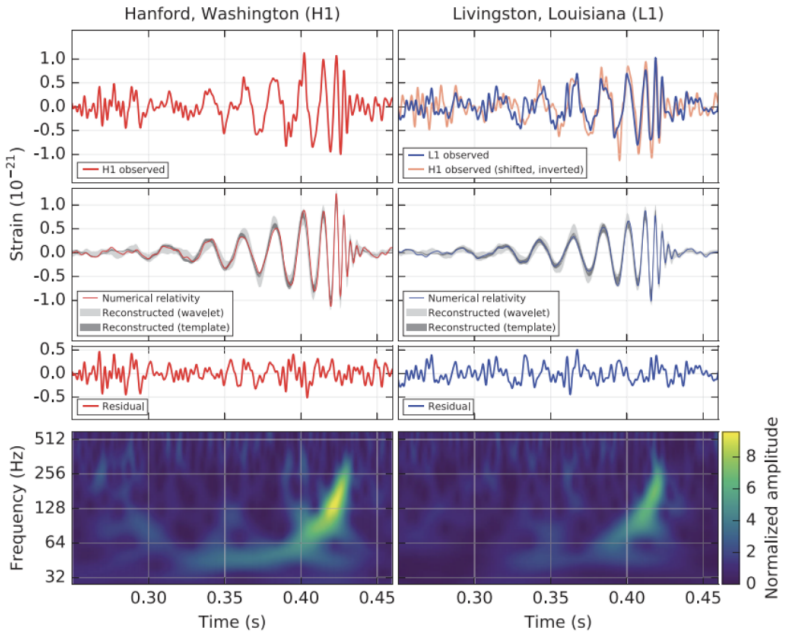

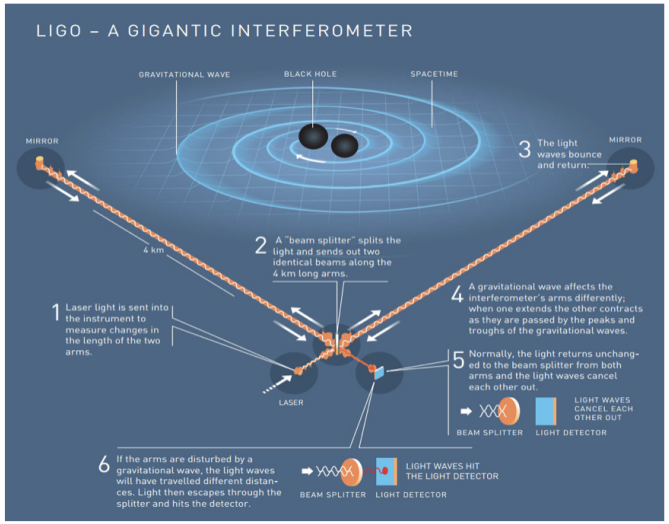

[15] [LIGO-Virgo Collaboration], *Phys. Rev. Lett.* **116**, 061102 (2016)

Gravitational spectrum (ground-based detectors)

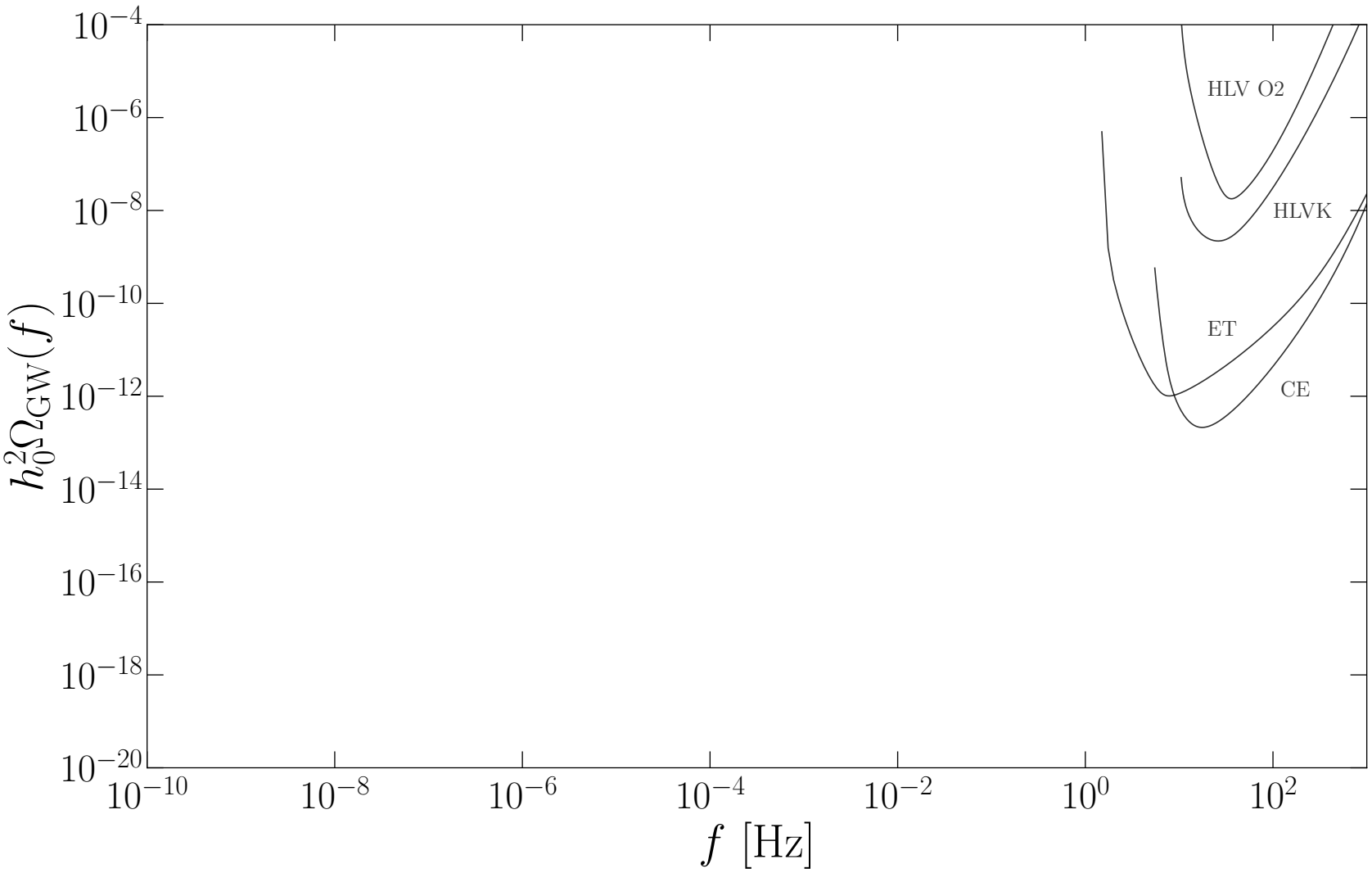

LISA

- Laser Interferometer Space Antenna (LISA) is a space–based GW detector
- Approved in 2017 as one of the main research missions of ESA (L3) with NASA collaboration
- Launch planned for 2035
- Composed by three spacecrafts in a distance of 2.5M km
- LISA cosmology working group (since 2015, $\sim$ 230 members)

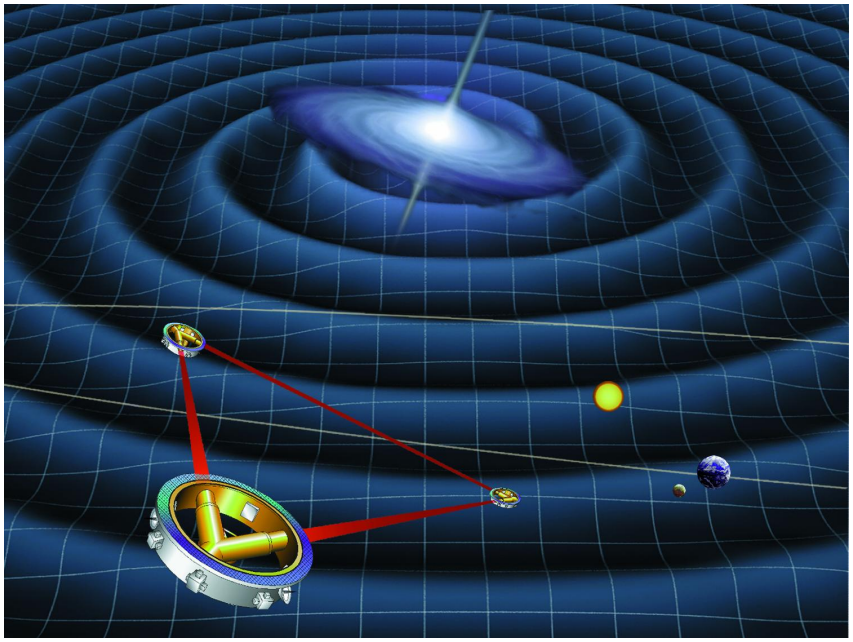

Figure: Artist's impression of LISA from Wikipedia

White paper:

[LISA Cosmology Working Group] (incl. ARP), *Living Rev. Rel.* **26** (2023), arXiv:2204.05434.

Pulsar Timing Array (PTA)
[see A. Mitridate's talk]

- An array of millisecond pulsars (MSP) is observed in the radio band to compute the delays on the time of arrival due to the presence of GWs.
- Collected data is the time series of residuals for each pulsar:

$$\delta t^i = t^i_{\rm obs} - t^i_{\rm TM}$$

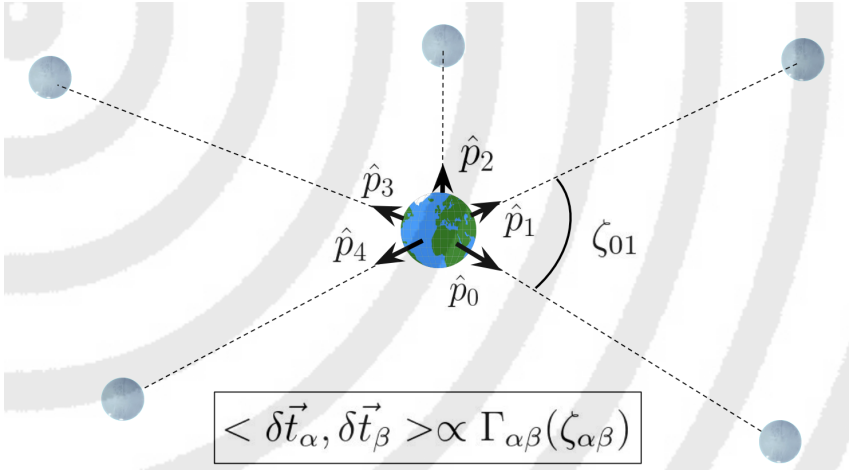

Credit: Mikel Falxa

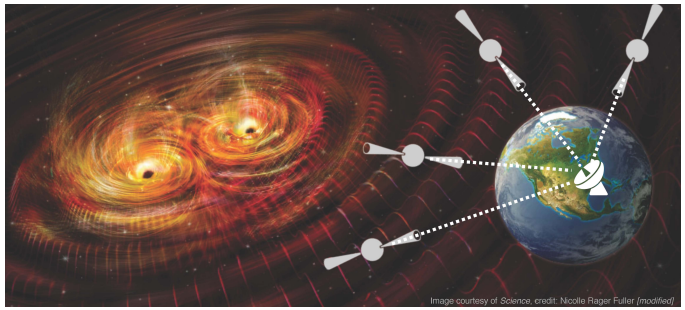

Figure: Image courtesy of Science, credit: Nicolle Rager Fuller

The correlation $\Gamma_{\alpha\beta}$ follows in GR the Hellings-Downs curve[16]

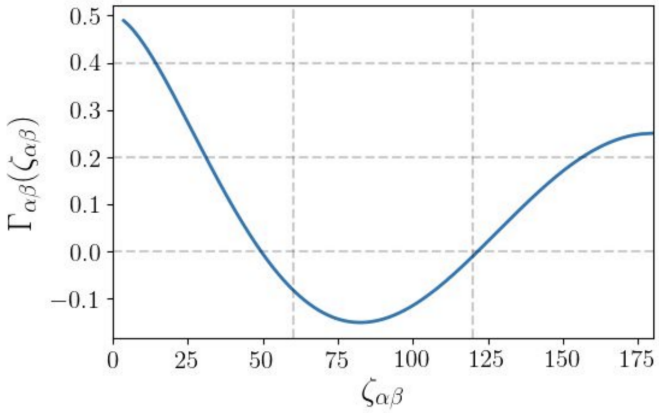

[16] R. W. Hellings and G. S. Downs, *Astrophys. J. Lett.* **265** (1983) L39-L42.

PTA detection [see A. Mitridate's talk]

- The PTA collaborations reported for the first-time evidence of a stochastic gravitational wave background on a press release on June 28, 2023 (plus a series of papers by each collaboration).

NANOGrav:
68 pulsars, 16yr of data
~3-4σ significance

Agazie et al. [2306.16213]

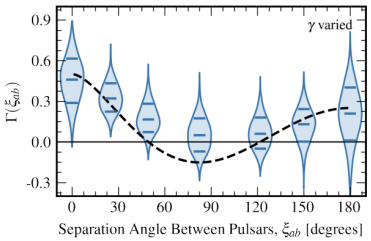

PPTA:
32 pulsars, 18yr of data
~2σ significance

Reardon et al. [2306.16215]

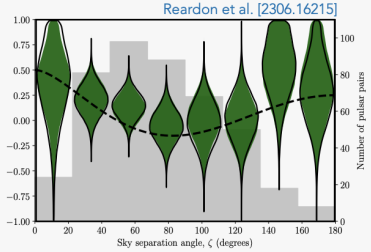

EPTA + InPTA:
25 pulsars, 24yr of data
~3σ significance

Antoniadis et al. [2306.16214]

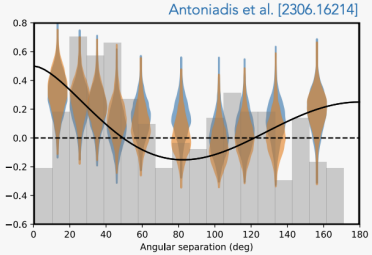

CPTA:
57 pulsars, 3yr of data
~4.6σ significance

Xu et al. [2306.16216]

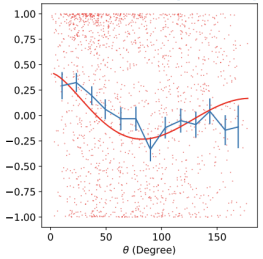

Credit: Andrea Mitridate

Probing the early Universe with GWs

Cosmological (pre-recombination) GW background

- Why background? Individual sources are not resoluble, superposition of single events occurring in the whole Universe.

$$f_* \simeq 1.64 \times 10^{-3} \frac{100}{R_* \mathcal{H}_*} \frac{T_*}{100\,\mathrm{GeV}}\,\mathrm{Hz}$$

- Phase transitions
  - Ground-based detectors (LVK, ET, CE) frequencies are 10–1000 Hz
    Peccei-Quinn, B-L, left-right symmetries $\sim 10^7, 10^8$ GeV.
  - Space-based detectors **(LISA)** frequencies are 10^{-5}–10^{-2} Hz
    Electroweak phase transition $\sim$ 100 GeV
  - Pulsar Timing Array **(PTA)** frequencies are 10^{-9}–10^{-7} Hz
    Quark confinement (QCD) phase transition $\sim$ 100 MeV

GW sources in the early Universe

- Magnetohydrodynamic (MHD) sources of GWs:
  - Sound waves generated from first-order phase transitions.
  - (M)HD turbulence from first-order phase transitions.
  - Primordial magnetic fields.

- High-conductivity of the early universe leads to a high-coupling between magnetic and velocity fields.

- Other sources of GWs include
  - Bubble collisions.
  - Cosmic strings.
  - Primordial black holes.
  - Inflation.

ARP *et al.*, 2307.10744, 2308.12943

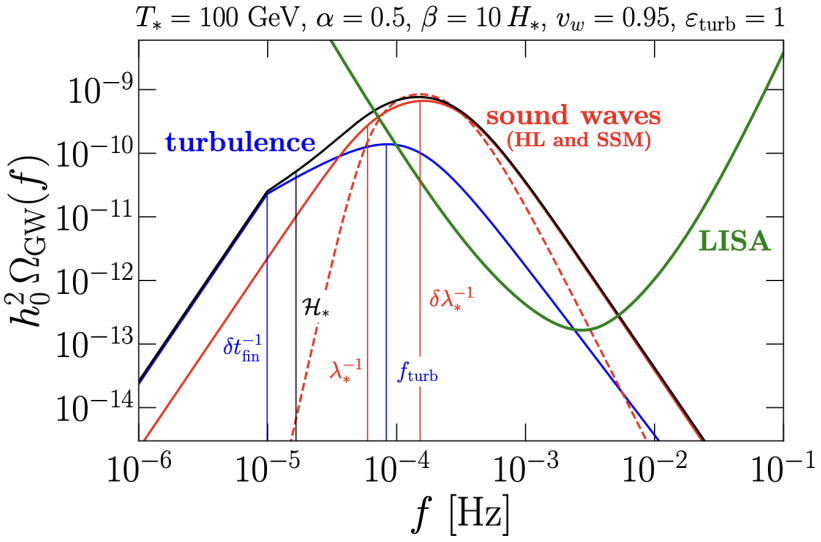

Gravitational spectrum (turbulence from PTs)[17]

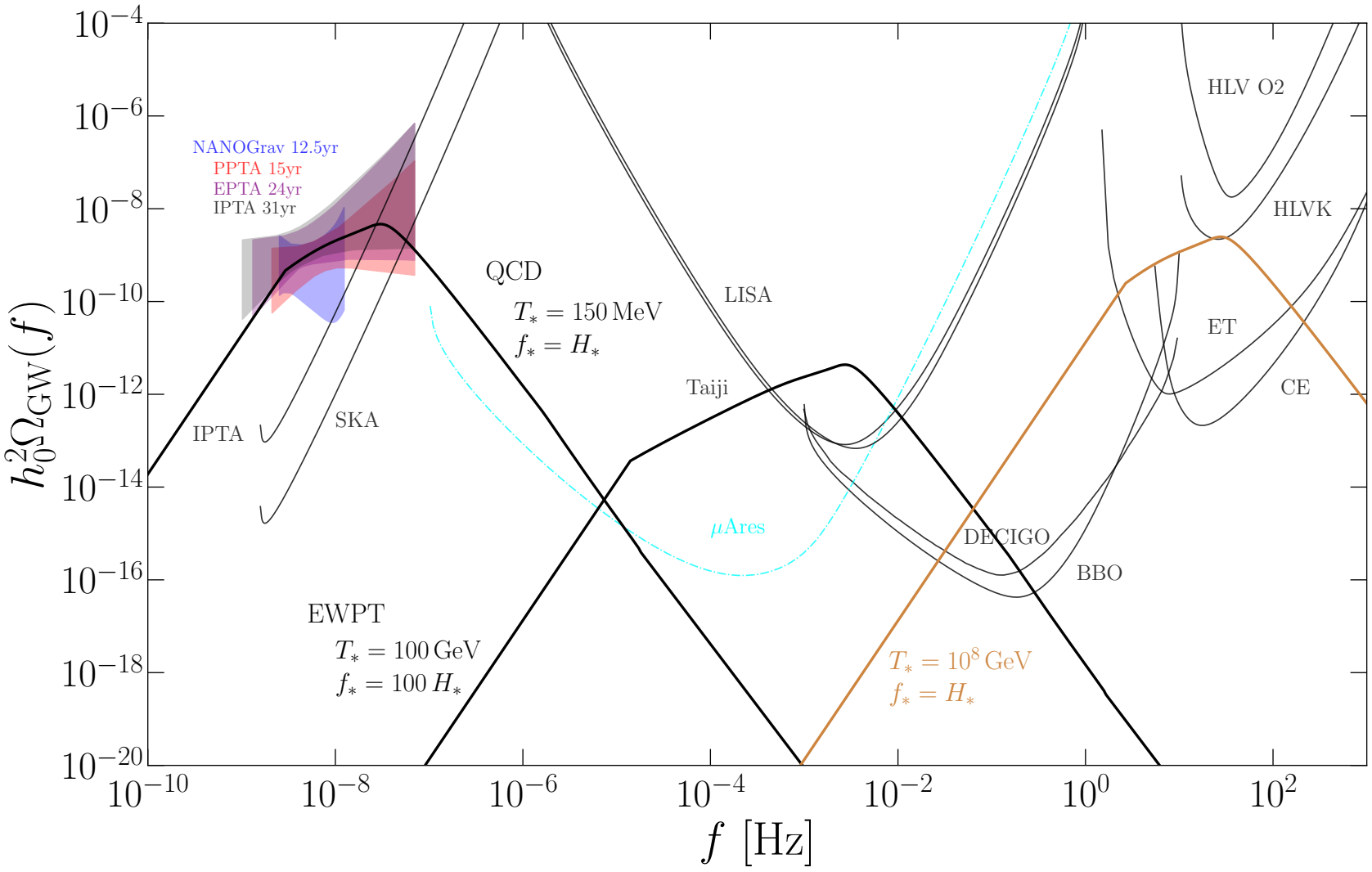

[17] ARP, C. Caprini, A. Neronov, D. Semikoz, *PRD* **105**, 123502 (2022)
A. Neronov, ARP, C. Caprini, D. Semikoz, *PRD* **103**, L041302 (2021)
ARP *et al.*, arXiv:2307.10744 (2023).

EPTA 24.7 yr data observation (DR 2)[18]

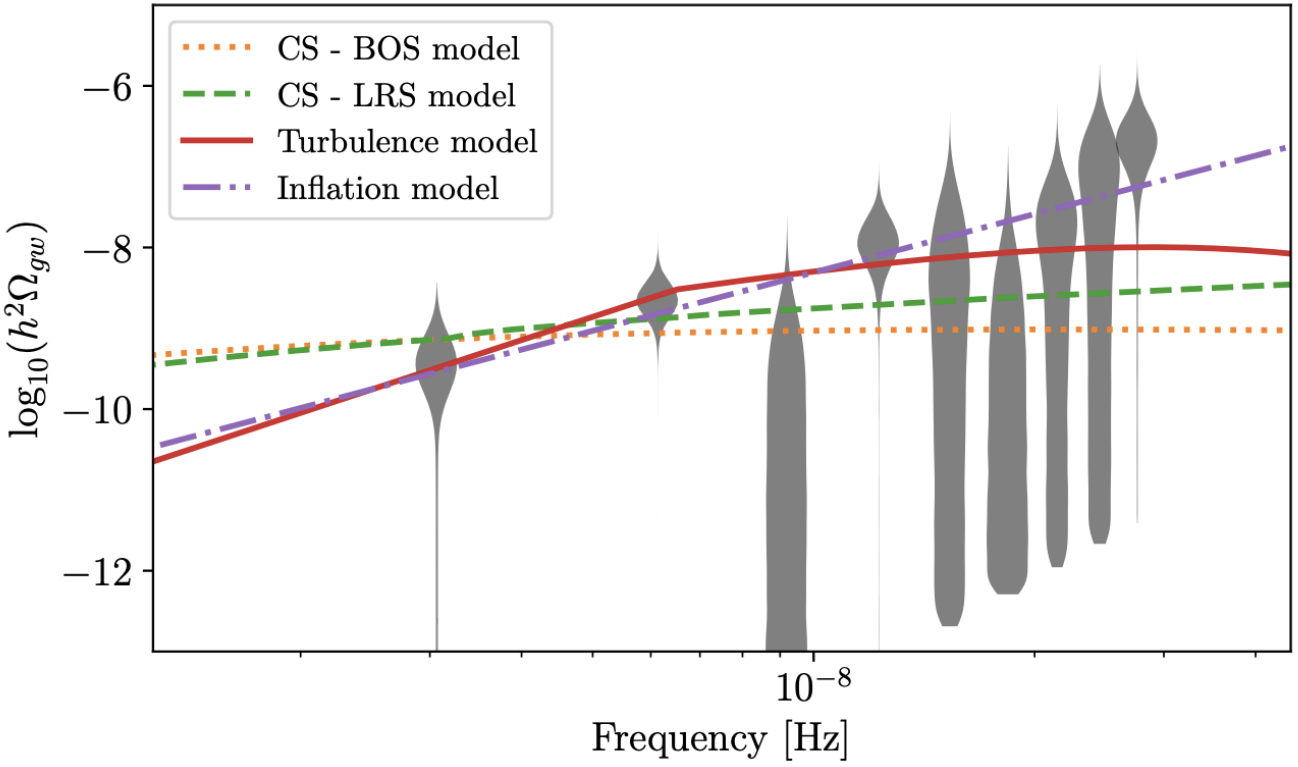

[18] [EPTA Collaboration] (incl. ARP), arXiv:2306.16227.

Primordial magnetic fields and GWs from MHD turbulence

- During the radiation-dominated era, after they are produced, magnetic fields will decay following MHD turbulence.
- Direct numerical simulations using the PENCIL CODE[19] to solve:
  1. Relativistic MHD equations adapted for radiation-dominated era (after electroweak symmetry is broken).
  2. Gravitational waves equation.
- In general, large-scale simulations are necessary to solve the MHD nonlinearities (e.g., unequal-time correlators UETC and non-Gaussianities, which require simplifying assumptions in analytical studies).
- Currently, $\mathcal{C}$osmo$\mathcal{L}$attice-MHD module is under-development (work with D. Figueroa, K. Marschall, A. Midiri).

[19] Pencil Code Collaboration, JOSS **6**, 2807 (2020), https://github.com/pencil-code/

MHD description

Right after the electroweak phase transition we can model the plasma using continuum MHD.

- Charge-neutral, electrically conducting fluid.
- Relativistic magnetohydrodynamic (MHD) equations.
- Radiation-dominated fluid

$$p = \rho c^2/3,$$

  i.e., $c_s^2 = 1/3$ (ultrarelativistic EoS).
- Friedmann–Lemaître–Robertson–Walker metric

$$g_{\mu\nu} = \mathrm{diag}\{-1, a^2, a^2, a^2\}$$

Conservation laws for MHD turbulence

$$T^{\mu\nu}{}_{;\nu} = 0, \quad F^{\mu\nu}{}_{;\nu} = -J^{\mu}, \quad \tilde{F}^{\mu\nu}{}_{;\nu} = 0$$

In the limit of subrelativistic bulk flow:

$$\gamma^2 \sim 1 + (v/c)^2 + \mathcal{O}(v/c)^4$$

Relativistic MHD equations are reduced to[20]

$$\begin{aligned}
\frac{\partial \ln \rho}{\partial t} &= -\frac{4}{3}\left(\nabla \cdot \boldsymbol{u} + \boldsymbol{u} \cdot \nabla \ln \rho\right) + \frac{1}{\rho}\left[\boldsymbol{u} \cdot (\boldsymbol{J} \times \boldsymbol{B}) + \eta \boldsymbol{J}^2\right], \\
\frac{D\boldsymbol{u}}{Dt} &= \frac{\mathbf{u}}{3}\left(\nabla \cdot \boldsymbol{u} + \boldsymbol{u} \cdot \nabla \ln \rho\right) - \frac{\boldsymbol{u}}{\rho}\left[\boldsymbol{u} \cdot (\boldsymbol{J} \times \boldsymbol{B}) + \eta J^2\right] \\
&\quad - \frac{1}{4}\nabla \ln \rho + \frac{3}{4\rho}\boldsymbol{J} \times \boldsymbol{B} + \frac{2}{\rho}\nabla \cdot (\rho\nu \boldsymbol{S}), \\
\frac{\partial \boldsymbol{B}}{\partial t} &= \nabla \times (\boldsymbol{u} \times \boldsymbol{B} - \eta \boldsymbol{J}), \quad \boldsymbol{J} = \nabla \times \boldsymbol{B},
\end{aligned} \tag{1}$$

for a flat expanding universe with comoving and normalized $p = a^4 p_{\rm phys}, \rho = a^4 \rho_{\rm phys}, B_i = a^2 B_{i,{\rm phys}}, u_i$, and conformal time t $(\mathrm{d}t = a\mathrm{d}t_c)$.

[20] A. Brandenburg, *et al.*, *Phys. Rev. D* **54**, 1291 (1996).
ARP, Midiri, *Relativistic Magnetohydrodynamics in the early Universe*, arXiv:2501.05732 (2025).

Evolution of magnetic strength and correlation length[21]

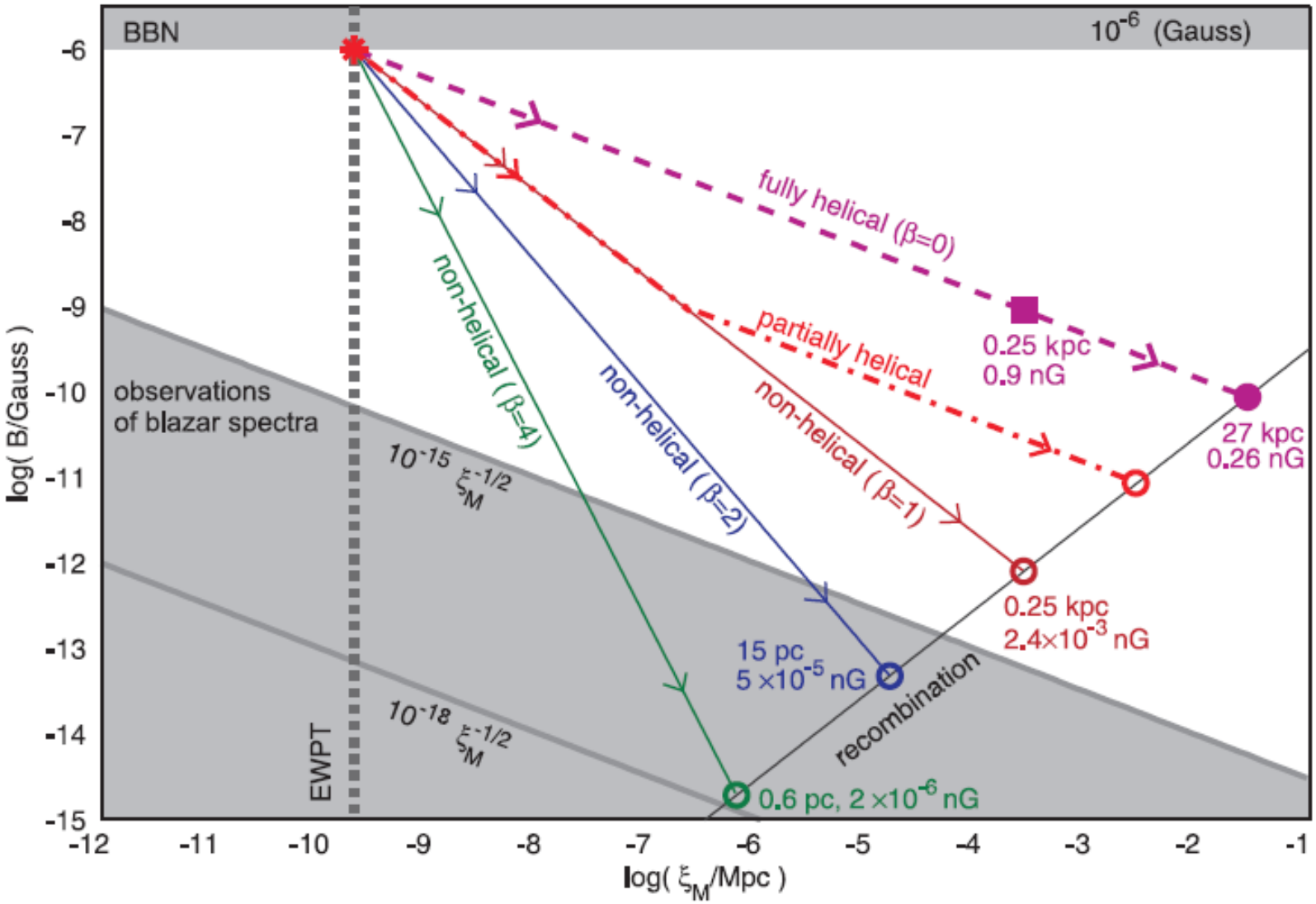

[21] A. Brandenburg *et al.* (incl. ARP), *Phys. Rev. D* **96**, 123528 (2017).

Numerical results for decaying MHD turbulence[22]

$1152^3, \Omega_{\mathrm{M}} \sim 10^{-2}$

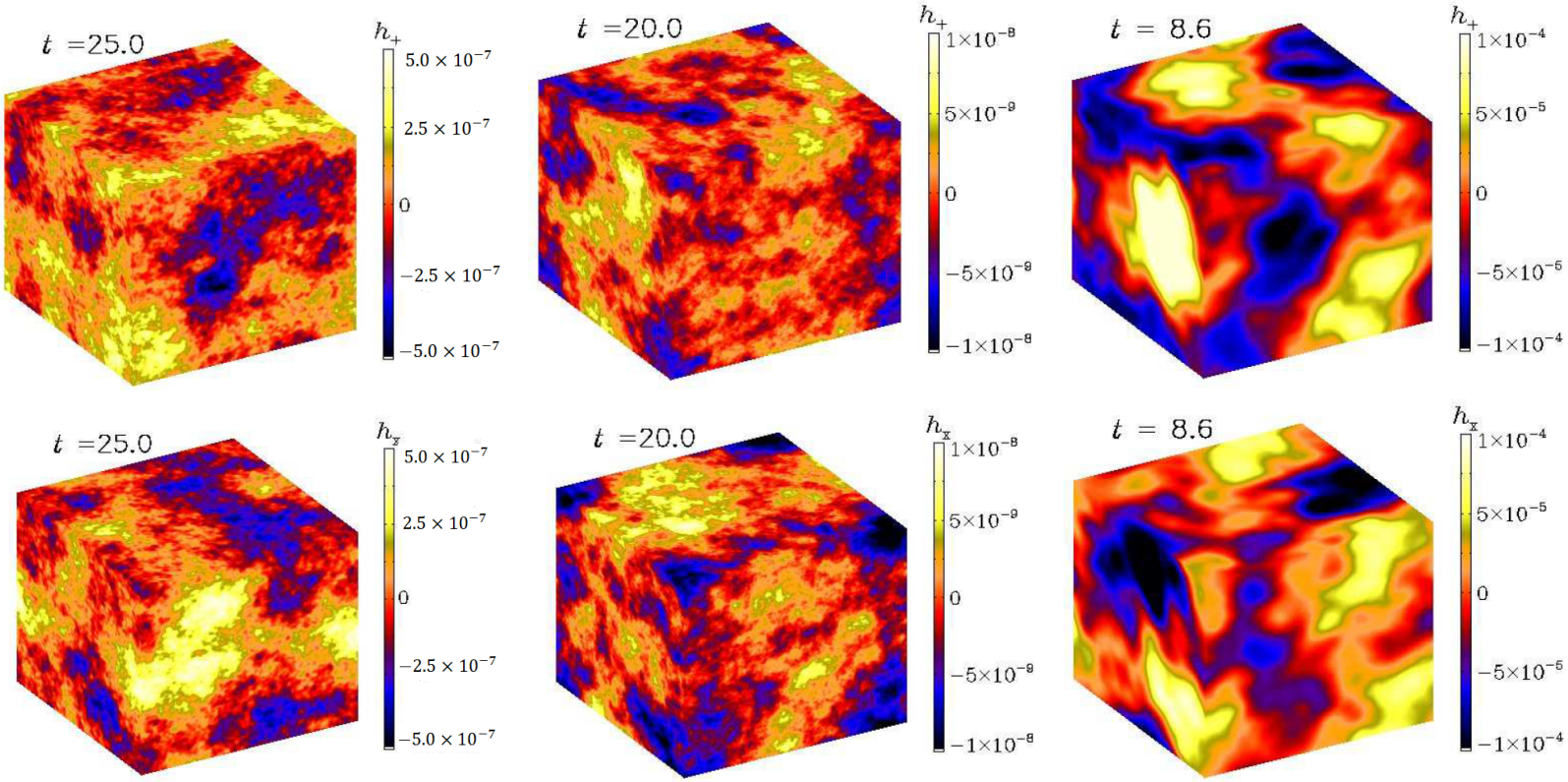

$k_{\mathrm{M}}/k_H = 300$ $k_{\mathrm{M}}/k_H = 60$ $k_{\mathrm{M}}/k_H = 2$

[22] ARP *et al.*, *Phys. Rev. D* **102**, 083512 (2020).

Numerical results for decaying MHD turbulence[23]

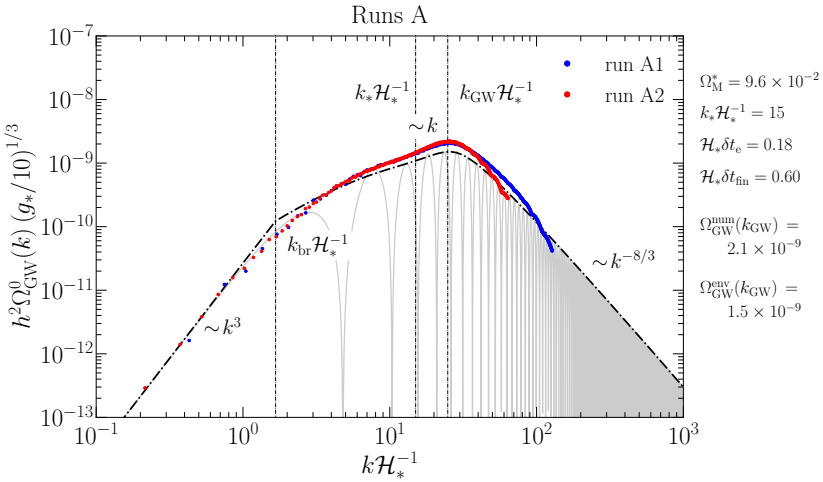

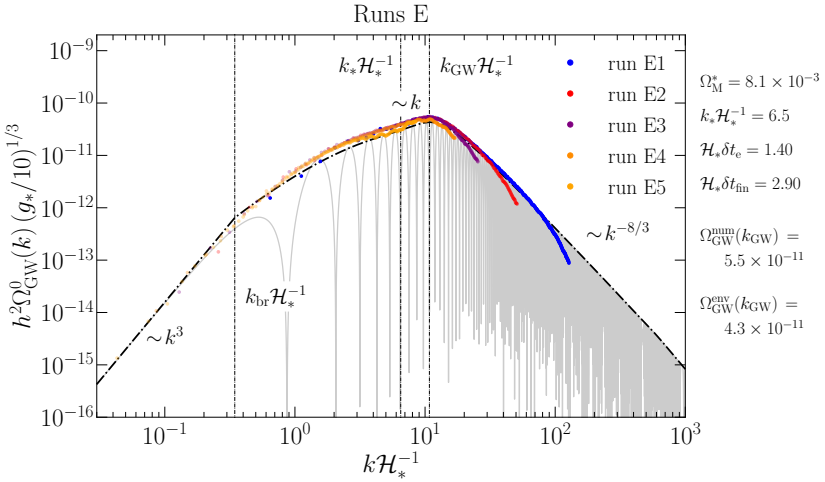

run	$\Omega_{\rm M}^*$	$k_*\mathcal{H}_*^{-1}$	$\mathcal{H}_*\delta t_e$	$\mathcal{H}_*\delta t_{\rm fin}$	$\Omega_{\rm GW}^{\rm num}(k_{\rm GW})$	$[\Omega_{\rm GW}^{\rm env}/\Omega_{\rm GW}^{\rm num}](k_{\rm GW})$	n	$\mathcal{H}_*L$	$\mathcal{H}_*t_{\rm end}$	$\mathcal{H}_*\eta$
A1	9.6×10^{-2}	15	0.176	0.60	2.1×10^{-9}	1.357	768	6π	9	10^{-7}
A2	–	–	–	–	–	–	768	12π	9	10^{-6}
E1	8.1×10^{-3}	6.5	1.398	2.90	5.5×10^{-11}	1.184	512	4π	8	10^{-7}
E2	–	–	–	–	–	–	512	10π	18	10^{-7}
E3	–	–	–	–	–	–	512	20π	61	10^{-7}
E4	–	–	–	–	–	–	512	30π	114	10^{-7}
E5	–	–	–	–	–	–	512	60π	234	10^{-7}

[23] ARP *et al.*, *Phys. Rev. D* **105**, 123502 (2022).

Analytical model for GWs from decaying turbulence

- Assumption: magnetic or velocity field evolution $\delta t_{\rm e} \sim 1/(u_* k_*)$ is slow compared to the GW dynamics ($\delta t_{\rm GW} \sim 1/k$) at all $k \gtrsim u_* k_*$.
- We can derive an analytical expression for nonhelical fields of the envelope of the oscillations[24] of $\Omega_{\rm GW}(k)$.

$$\Omega_{\rm GW}(k, t_{\rm fin}) \approx 3 \left(\frac{k}{k_*}\right)^3 {\Omega_{\rm M}^*}^2 \frac{\mathcal{C}(\alpha)}{\mathcal{A}^2(\alpha)}\, p_\Pi\left(\frac{k}{k_*}\right) \times \begin{cases} \ln^2[1 + \mathcal{H}_* \delta t_{\rm fin}] & \text{if } k\,\delta t_{\rm fin} < 1, \\ \ln^2[1 + (k/\mathcal{H}_*)^{-1}] & \text{if } k\,\delta t_{\rm fin} \geq 1. \end{cases}$$

- p_Π is the anisotropic stress spectrum and depends on spectral shape, can be approximated for a von Kárman spectrum as[25]

$$p_\Pi(k/k_*) \simeq \left[1 + \left(\frac{k}{2.2 k_*}\right)^{2.15}\right]^{-11/(3\times 2.15)}$$

[24] ARP *et al.*, *Phys. Rev. D* **105**, 123502 (2022).

[25] ARP *et al.*, arXiv:2307.10744 (2023).

Multi-messenger studies of primordial magnetic fields[30]

- Primordial magnetic fields would evolve through the history of the universe up to the present time and could explain the lower bounds in cosmic voids derived by the Fermi collaboration.[31]

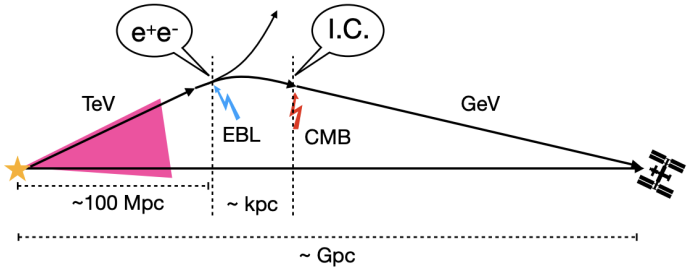

- Maximum amplitude of primordial magnetic fields is constrained by the big bang nucleosynthesis.[32]

- Additional constraints from CMB, Faraday Rotation, ultra-high energy cosmic rays (UHECR).

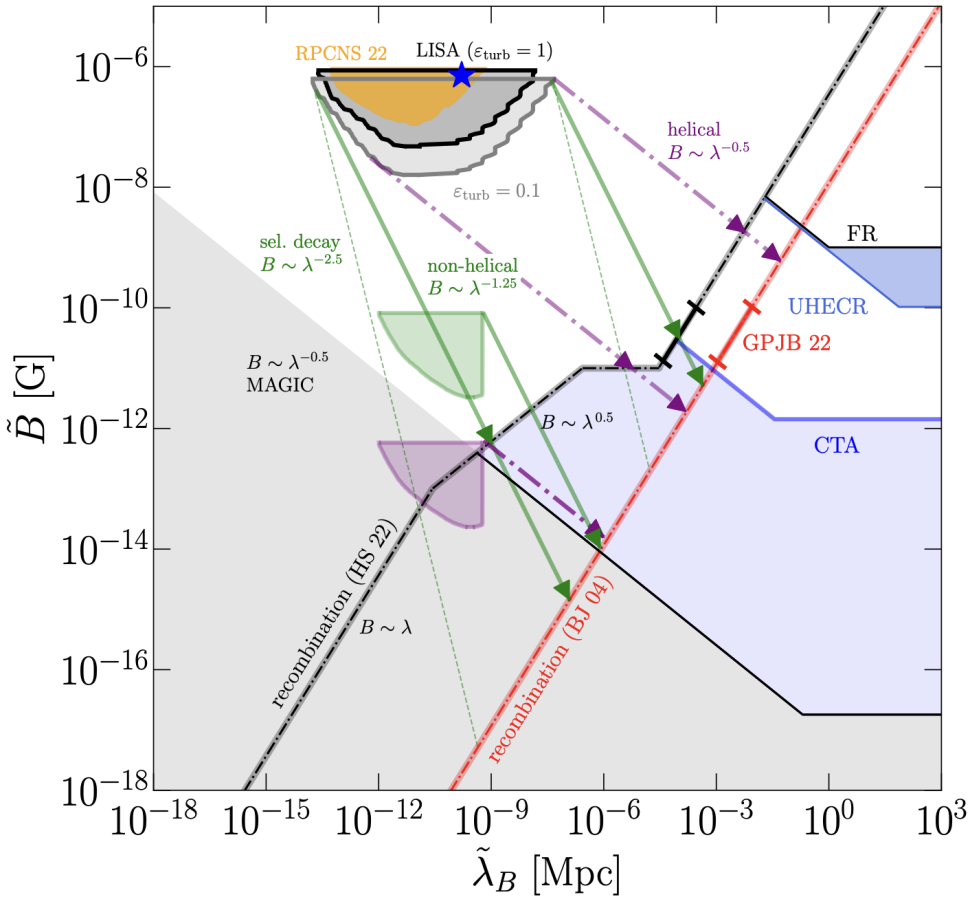

[30] ARP *et al.*, arXiv:2307.10744 (2023).
[31] A. Neronov and I. Vovk, *Science* **328**, 73 (2010).
[32] V. F. Shvartsman, *Pisma Zh. Eksp. Teor. Fiz.* **9**, 315 (1969).

Primordial magnetic field constraints with PTA[26]

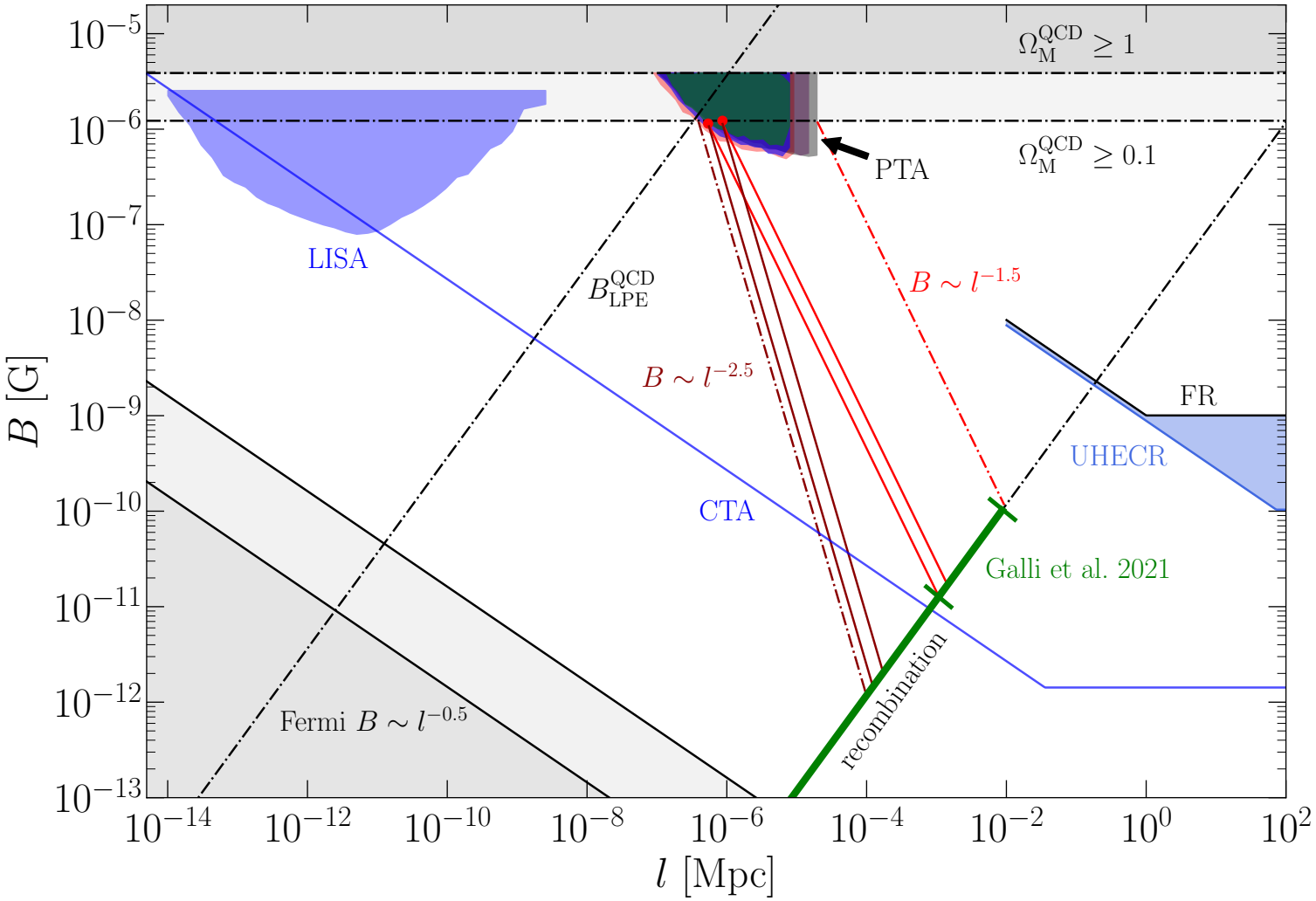

[26] ARP *et al.*, *Phys. Rev. D* **105**, 123502 (2022).

Conclusions

- Magnetic fields are ubiquitous in nature at all scales, from the smallest structures up to galaxies, cluster of galaxies, filaments, and potentially in cosmic voids of the LSS.
- Observations from γ-rays indicate the presence of intergalactic magnetic fields that could have their origin in the early Universe and potentially alleviate the Hubble tension.
- Magnetic fields can be produced in the early Universe during the period of inflation or during a cosmological phase transition (EW or QCD), leaving at the same time an imprint on the gravitational wave background (GWB).
- The large conductivity during the radiation-dominated era implies the development of MHD turbulence and therefore, the primordial plasma is non-linearly stirred by the magnetic field.
- LISA, PTA, and next-generation ground-based detectors can be used to probe the origin of magnetic fields in the largest scales of our Universe, which is still an open question in cosmology.
- In summary, magnetic fields can be used as multi-messenger probes for early Universe physics combining astrophysical and cosmological observations, and can help us understanding high-energy physics, at scales inaccessible by other means.

Thank You!

alberto.roperpol@unige.ch

github.com/AlbertoRoper/cosmoGW

cosmology.unige.ch/users/alberto-roper-pol

CosmoLattice — School 2025 —

CosmoLattice School 2025 (IBS, Korea), Sept 22-26

This school offers a pedagogical introduction to lattice field theory techniques and their application to the simulation of interacting fields in an expanding Universe. Participants will also be introduced to CosmoLattice, an open-access code designed for such simulations. The school will provide a comprehensive guide to using CosmoLattice for modeling the non-linear dynamics of scalar and gauge fields in cosmological contexts.

The school is aimed to anyone who would like to learn (or simply improve their knowledge on) how to simulate in a lattice the dynamics of early Universe field theory scenarios. Topics covered include:

- **Lattice field theory techniques**: discretization schemes, lattice gauge techniques, and more
- **Numerical algorithms for differential equations**: Leapfrog, Verlet, Runge-Kutta, etc
- **Overview of CosmoLattice**: libraries, modularity, parallelization, ...
- **Lattice simulations of interacting fields in an expanding background**:
  - Scalar field dynamics with arbitrary potentials
  - U(1) gauge theories coupled to complex charged scalars
  - SU(2) gauge theories coupled to doublet charged scalars
- **Modern applications to early Universe scenarios**:
  - Preheating scenarios and onset of radiation domination
  - Production and evolution of gravitational waves
  - Dynamics of derivatively coupled Axion-like fields
  - Dynamics of non-minimally coupled scalar fields
  - Fluid dynamics and gravitational waves from turbulence
  - Evolution and experimental signatures of topological defects

Registration is open until August 31st

Lecturers:

J. Baeza-Ballesteros ..... DESY, Zeuthen, Germany
D. G. Figueroa ..... IFIC, Valencia, Spain
N. Loayza ..... IFIC, Valencia, Spain
K. Marschall ..... IFIC, Valencia, Spain
A. S. Midiri ..... University of Geneva, Switzerland
T. Opferkuch ..... SISSA, Trieste, Italy
A. Roper Pol ..... University of Geneva, Switzerland
B. A. Stefanek ..... IFIC, Valencia, Spain
F. Torrenti ..... University of Barcelona, Barcelona, Spain
A. Urio ..... UPV/EHU, Bilbao, Spain

Pencil Code school and user meeting

Oct 20 – 31, 2025
CERN

Pencil Code (http://pencil-code.nordita.org/) is a modular MPI public code to efficiently solve coupled systems of partial differential equations in high-performance computing architectures using high-order finite-difference schemes. Started in 2001 by A. Brandenburg and W. Dobler, its core application initially focused on magnetohydrodynamics (MHD) for solar physics. Since then, it has been continuously under development by a total of 90 contributors covering a broad range of applications.

In particular, it has been used for studies of early universe physics including the evolution and formation of primordial magnetic fields and chiral MHD; the production of gravitational waves and propagation of gravitational waves in modified gravity, and inflation.

1st Pencil Code school on early Universe physics and gravitational waves (Oct 20-24)

The Pencil Code school on early Universe physics and gravitational waves will take place on October 20-24 as part of a two-week CERN TH institute.

The school targets early-career and senior researchers that are interested in learning and developing numerical skills applied to early Universe physics using Pencil Code.

The lectures will cover numerical aspects:

- *Introduction to Pencil Code*
- *Finite-difference schemes for partial differential equations*
- *Post-processing of data with IDL and Python*
- *GPU acceleration of Pencil Code*

as well as applications to particular physics cases with hands-on exercises on:

- *Magnetohydrodynamics of the early Universe*
- *Generation and evolution of primordial magnetic fields*
- *Chiral magnetohydrodynamics*
- *First-order phase transitions*
- *Gravitational wave production*
- *Axion inflation*

Lecturers: *Registration is open until September 10th*

- Axel Brandenburg (Nordita)
- Philippe Bourdin (University of Graz)
- Simon Candelaresi (University of Augsburg)
- Deepen Garg (University of Bonn)
- Frederick Gent (Aalto University & Nordita)
- Matthias Rheinhardt (Aalto University)
- Alberto Roper Pol (University of Geneva)
- Isak Stomberg (IFIC, Valencia)

21st Pencil Code user meeting PCUM2025 (Oct 27-31)

The Pencil Code user meeting will take place on October 27-31 as part of a two-week CERN TH institute.

Registration for the Pencil Code user meeting is open and will close on ***September 28th***.

Extra slides

Electroweak phase transition (first order?)

- Electroweak phase transition: symmetry of massless electroweak bosons is broken.
- Production of W^+, W^- and Z^0 mass bosons (weak force), and photons γ (EM).
- Standard Model predicts a smooth crossover[27] at a critical temperature of 159.5 ± 1.5 GeV for $m_{\mathrm{H}} = 125$ GeV.

Standard Model phase diagram

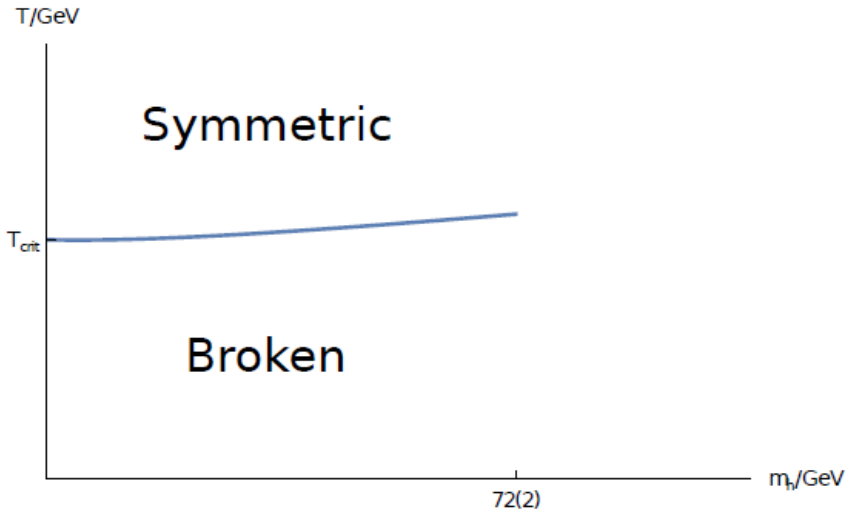

[27] K. Kajantie, M. Laine, K. Rummukainen, M. Shaposhnikov, *Nucl. Phys.* **466**, 189–258 (1996).

First–order electroweak phase transition

- SM extensions: singlet or triplet scalar extensions, two Higgs doublet, higgs portals, composite Higgs, scale invariant scalar extensions, SUSY models, low scale higher dimension operators.

- BSM additions are motivated by electroweak baryogenesis (Sakharov conditions, 1967).

  1. C and CP violation: particles scattering off the bubble walls, producing asymmetries.
  2. Baryon number violation: sphaleron transitions in front of the wall are biased to produce more baryons than antibaryons.
  3. Out of equilibrium: the bubble walls disturb the symmetric-phase equilibrium state.

First–order phase transition

$$V(\phi, T) = \frac{1}{2}M^2(T)\phi^2 - \frac{1}{3}\delta(T)\phi^3 + \frac{1}{4}\lambda\phi^4$$

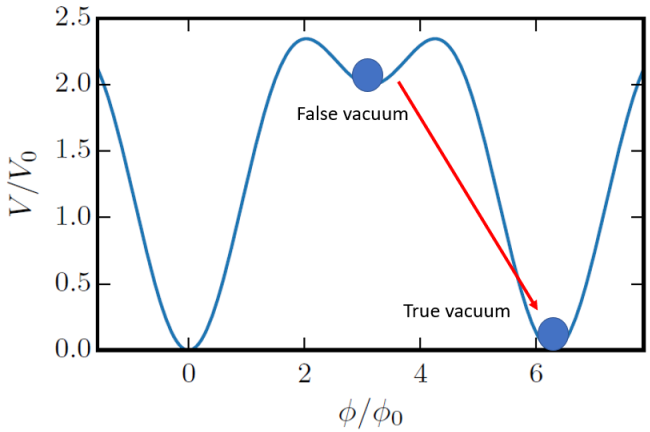

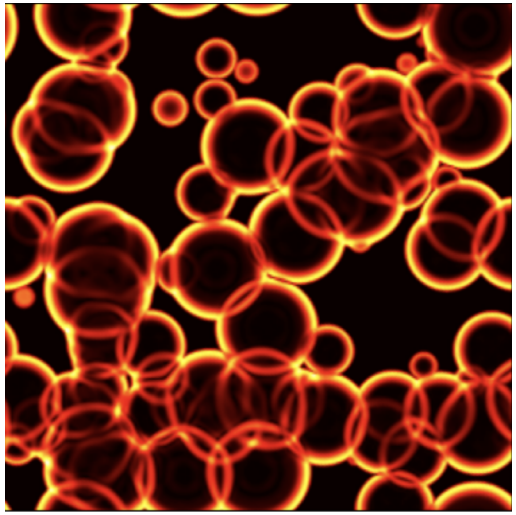

Credits: I. Stomberg

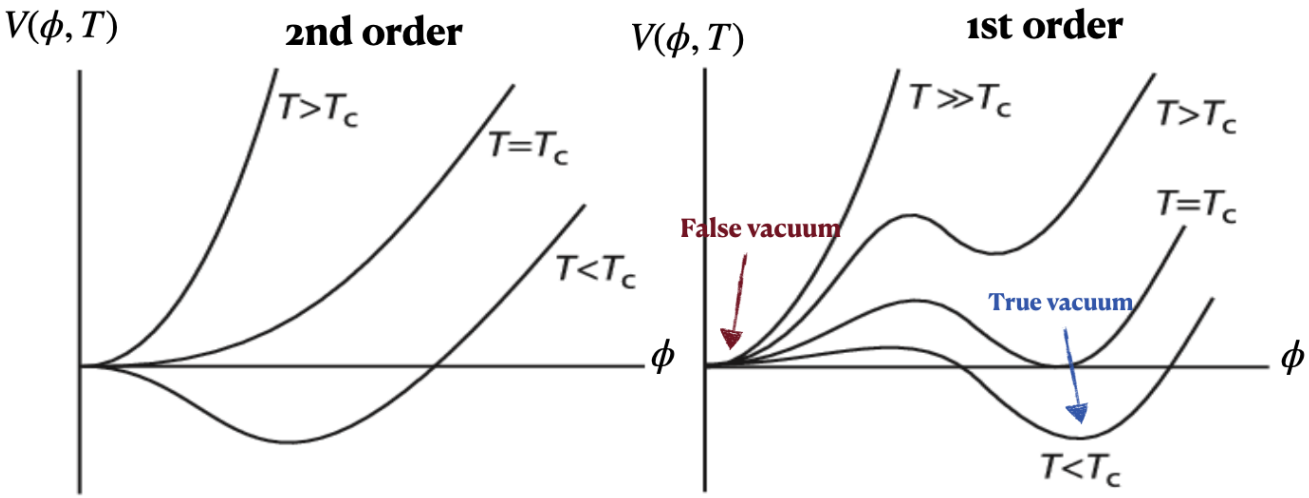

Hydrodynamics of first-order phase transitions[28]

- Broken-phase bubbles are nucleated and expand
- Friction from particles yield a terminal velocity ξ_w of the bubbles
- The bubble can run away when the friction is not enough to stop the bubble's acceleration

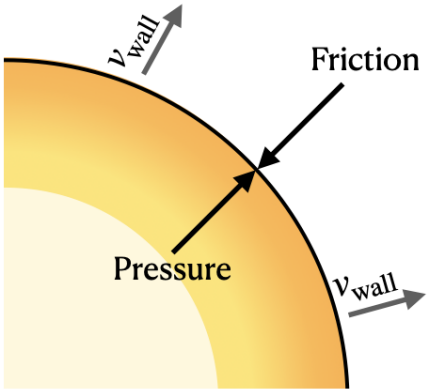

$$\nabla_\mu T^{\mu\nu}_{\rm field} = \frac{\partial V}{\partial \phi}\partial^\nu \phi + \eta u^\mu \partial_\mu \phi \partial^\nu \phi\,,$$

$$\nabla_\mu T^{\mu\nu}_{\rm fluid} = -\frac{\partial V}{\partial \phi}\partial^\nu \phi - \eta u^\mu \partial_\mu \phi \partial^\nu \phi\,,$$

[28] Espinosa, Konstandin, No, Servant, *JCAP* **06** (2010) 028.

GWs from sound waves: Higgsless simulations[29]

- Difficulty on simulations is due to the different scales of the scalar field ϕ and the fluid shell, so one can consider a nucleation history and set the pressure and energy density by knowing the value of ϵ and setting it during the simulation.
- Effect of bubble collisions on GWs is subdominant when sound waves are produced, so one can ignore the scalar field.
- Nucleation history is produced from an exponential probability distribution $P(t) \propto \exp\left[\beta(t - t_*)\right]$.

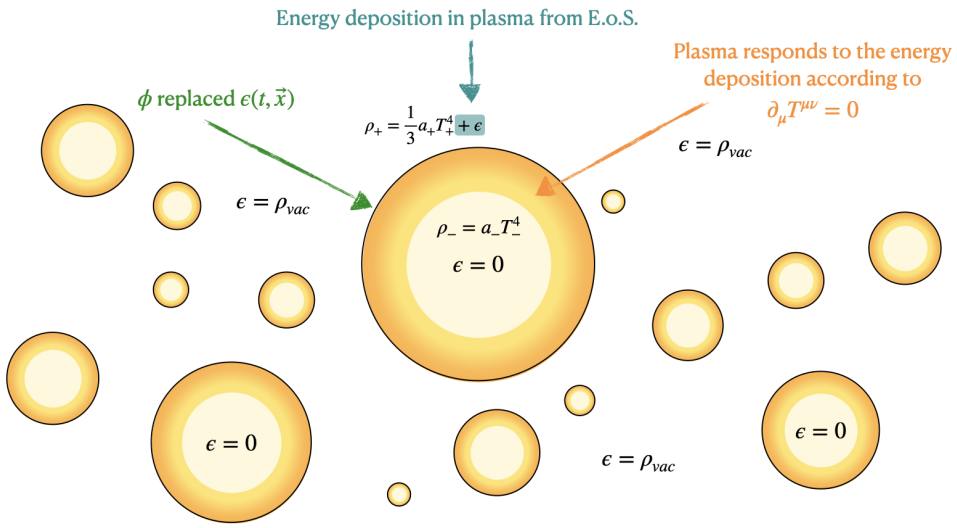

Credit: I. Stomberg

[29] Jinno *et al.* JCAP 02 (2023) 011, 2209.04369,
ARP, Stomberg et al., arXiv:2409.03651 (2024).

Higgsless simulations of strong PTs[30]

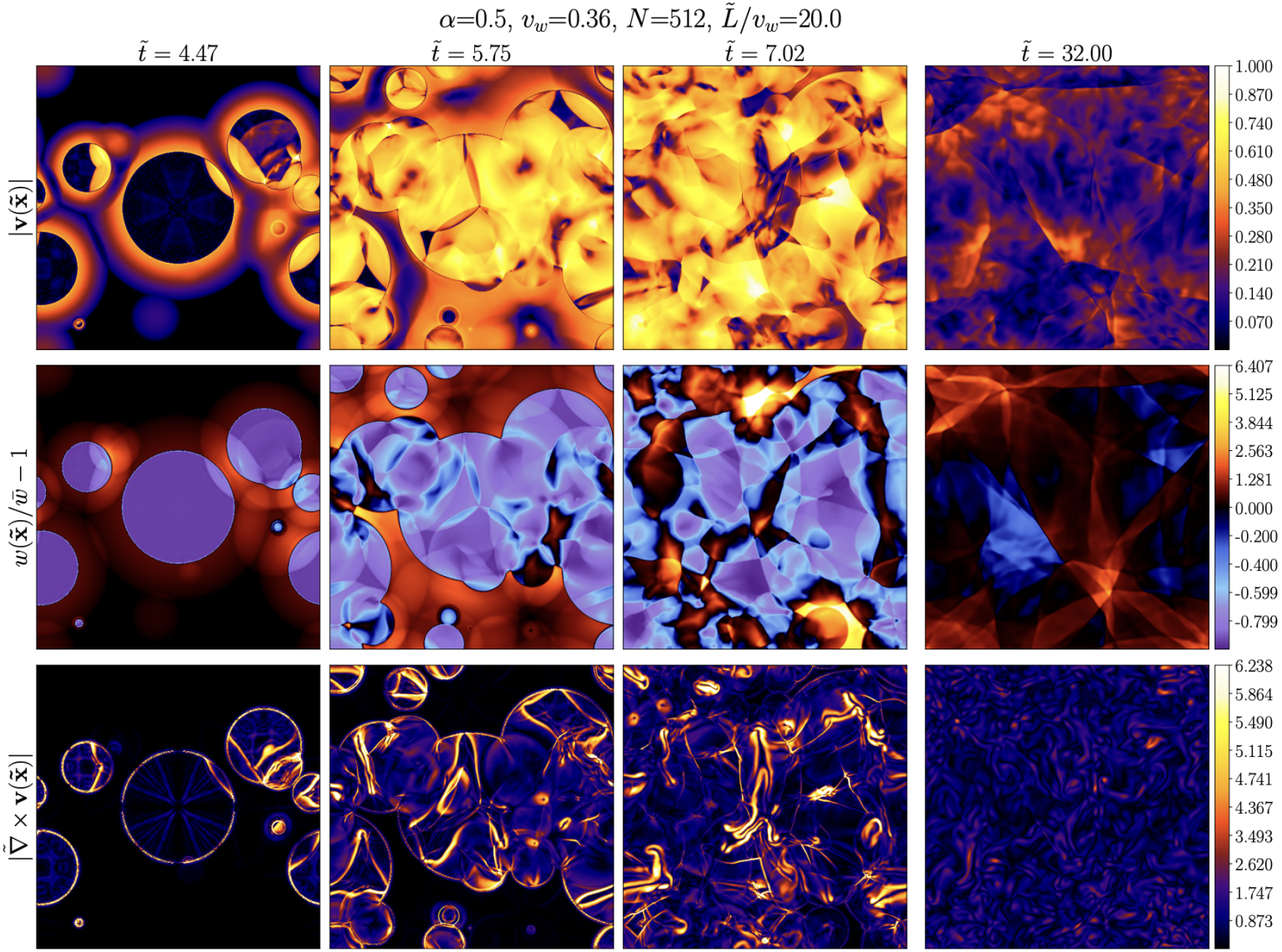

[30] ARP, Stomberg et al., arXiv:2409.03651.

Higgsless simulations (results)[31]

- In the literature, the GW spectrum from sound waves is usually assumed to be

$$\Omega_{\rm GW}(f) = 3\,\tilde{\Omega}_{\rm GW}\,K^2\,(H_*\tau_{\rm sw})\,(H_*R_*)\,S(f\,R_*)$$

- $\tilde{\Omega}_{\rm GW}$ is the efficiency factor

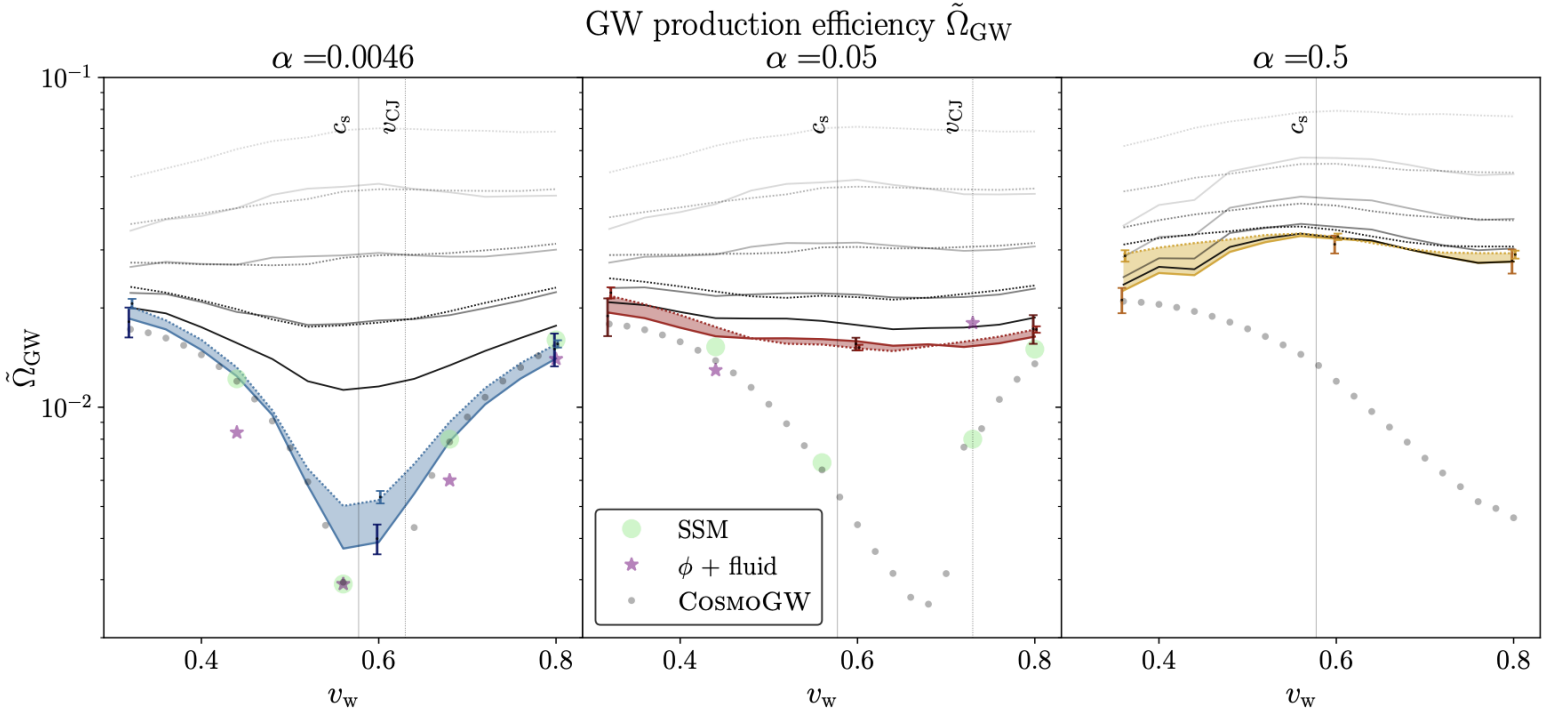

[31] ARP, Stomberg et al., arXiv:2409.03651 (2024).

Higgsless simulations (results)[32]

- Kinetic energy decay is observed in the simulations.
- For weak and strong PTs, increasing discretization enhances the decay.
- Potential indication of the development of non-linearities (turbulence).

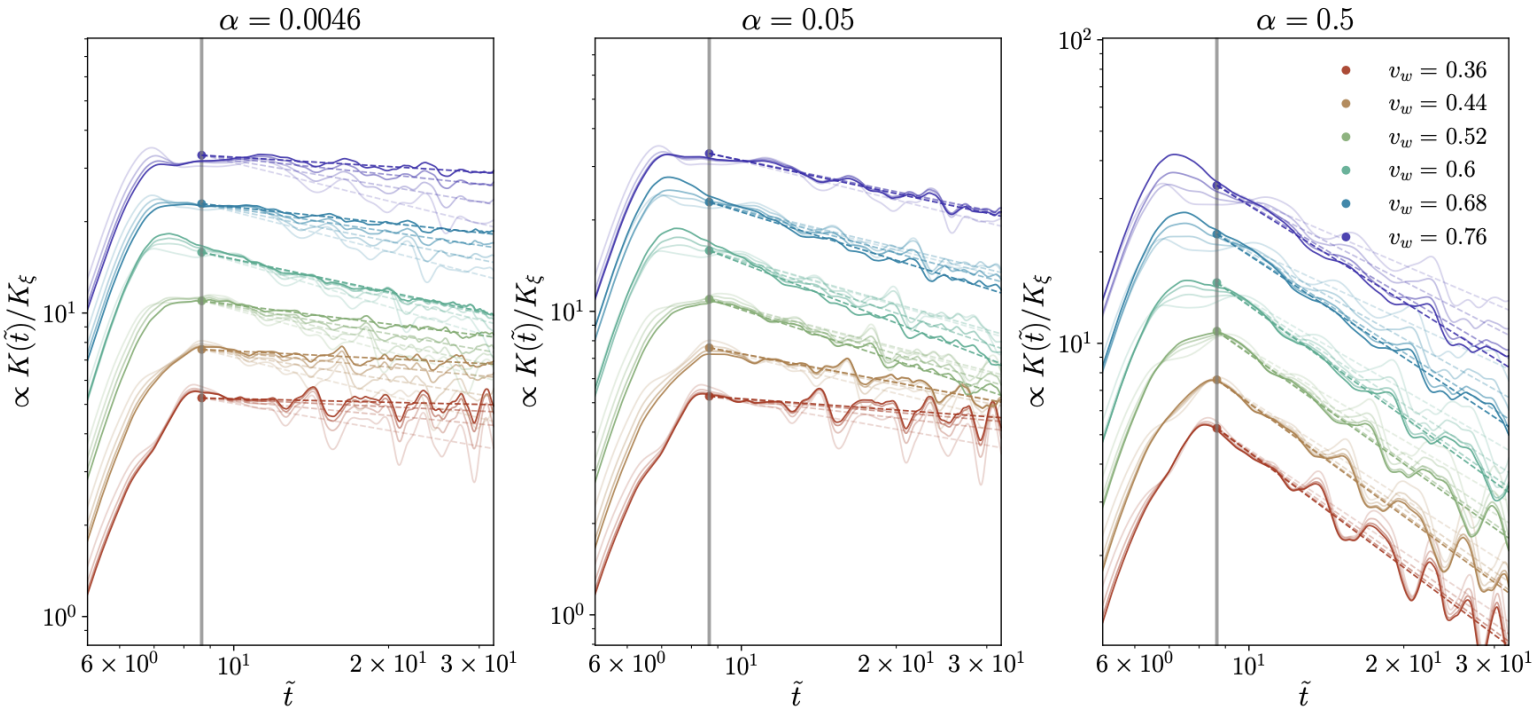

[32] ARP, Stomberg et al., arXiv:2409.03651 (2024).

Higgsless simulations (results)[33]

- In the literature, the GW spectrum from sound waves is usually assumed to be

$$\Omega_{\rm GW}(f) = 3\,\tilde{\Omega}_{\rm GW}\,K^2\,(\mathbf{H}_*\tau_{\rm sw})\,(H_*R_*)\,S(f\,R_*)$$

- The linear growth, which only appears when expansion is neglected, is modified when the decay of the source is significant (e.g., due to the development of non-linearities).
- Extended model to proposed locally stationary UETC

$$\Omega_{\rm GW}(f) = 3\,\tilde{\Omega}_{\rm GW}\,\mathbf{K}^2_{\rm int}\,(H_*R_*)\,S(f\,R_*)$$

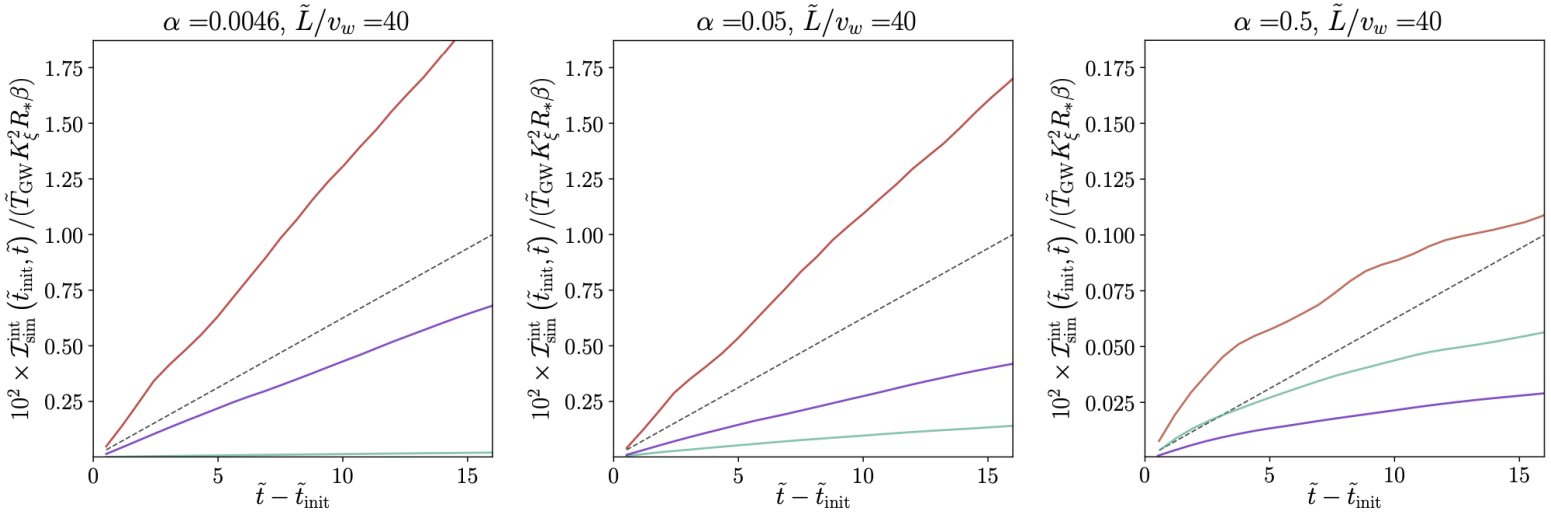

[33] ARP, Stomberg et al., arXiv:2409.03651 (2024).

Contributions to the stress-energy tensor from MHD sources

$$T^{\mu\nu} = \left(p/c^2 + \rho\right) U^\mu U^\nu + p g^{\mu\nu} + \pi^{\mu\nu} + F^{\mu\gamma} F^{\nu}{}_{\gamma} - \frac{1}{4} g^{\mu\nu} F_{\lambda\gamma} F^{\lambda\gamma}$$

- From fluid motions:

  $$T_{ij} = \left(p/c^2 + \rho\right) \gamma^2 u_i u_j + p\delta_{ij}$$

  - Ultrarelativistic EoS: $p = \rho c^2/3$
  - Viscous stresses: $\pi_{ij} = \nu(p/c^2 + \rho)(u_{i,j} + u_{j,i})$

- From magnetic fields:

  $$T_{ij} = -B_i B_j + \delta_{ij} B^2/2$$

- 4–velocity $U^\mu = \gamma(c, u^i)$
- 4–potential $A^\mu = (\phi/c, A^i)$

- 4–current $J^\mu = (c\rho_{\mathrm{e}}, J^i)$
- Faraday tensor $F_{\mu\nu} = \partial_\mu A_\nu - \partial_\nu A_\mu$

Conformal invariance of MHD equations[34]

An important aspect of the conservation laws of perfect fluids is that they are conformally invariant when the trace of the stress-energy tensor vanishes [10, 12]. To show this result, let us consider two metrics that are related by a conformal transformation as $g^{\mu\nu} = \Omega^2(x^\mu)\,\tilde{g}^{\mu\nu}$. This corresponds, for example, to the FLRW metric tensor $g^{\mu\nu}$ when we express the time coordinate as conformal time, where $\tilde{g}^{\mu\nu} = \eta^{\mu\nu}$ would correspond to flat Minkowskian space-time and $\Omega = a^{-1}(\tau)$ is the inverse scale factor. The conservation laws for a symmetric $T^{\mu\nu}$ given in a metric tensor $g^{\mu\nu}$ are

$$\begin{aligned} D_\mu T^{\mu\nu} &= \frac{1}{\sqrt{-g}}\partial_\mu\big(\sqrt{-g}\,T^{\mu\nu}\big) + \Gamma^\nu{}_{\mu\sigma}T^{\mu\sigma} \\ &= \frac{\Omega^4}{\sqrt{-\tilde{g}}}\partial_\mu\big(\sqrt{-\tilde{g}}\,\Omega^{-4}\,T^{\mu\nu}\big) + \tilde{\Gamma}^\nu{}_{\mu\sigma}T^{\mu\sigma} - 2\,T^{\mu\nu}\partial_\mu \ln\Omega + T^\mu_{\ \mu}\,\partial^\nu \ln\Omega\,, \end{aligned} \tag{3.13}$$

where $\tilde{\Gamma}^\nu{}_{\mu\sigma}$ are the Christoffel symbols of the metric tensor $\tilde{g}^{\mu\nu}$. Introducing the comoving stress-energy tensor $\tilde{T}^{\mu\nu} = \Omega^{-6}\,T^{\mu\nu}$, we find

$$D_\nu T^{\mu\nu} = 0 \Leftrightarrow D_{\tilde{\nu}}\tilde{T}^{\mu\nu} + \Omega^{-2}\,\tilde{T}^\nu{}_\nu\,\partial^\mu \ln\Omega = 0\,, \tag{3.14}$$

where $D_{\tilde{\nu}}$ is the covariant derivative in the metric tensor $\tilde{g}^{\mu\nu}$.

$$\tilde{T} = 3\tilde{p} - \tilde{\rho}$$

[34] ARP, Midiri, *Relativistic Magnetohydrodynamics in the early Universe*, arXiv:2501.05732 (2025)
Subramanian & Barrow, Phys.Rev.**D** 58 (1998) 083502

Initial conditions

Fractional helicity σ_{M} and peak frequency k_{M}

$$\varepsilon_{\mathrm{M}} = \frac{kH_{\mathrm{M}}(k,t)}{2E_{\mathrm{M}}(k,t)} = \frac{2\sigma_{\mathrm{M}}}{1+\sigma_{\mathrm{M}}^2}$$

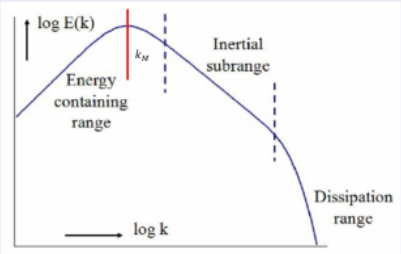

Ratio of energy densities

$$Q_* = \frac{B_*}{\sqrt{\rho_*}\,u_*}, \quad \text{where } t_* \text{ is the time of generation}$$

Three cases:

- $Q_* \gg 1$: Magnetically dominant turbulence ($E_{\mathrm{M}} \propto k^{\alpha_{\mathrm{M}}}$, $\alpha_{\mathrm{M}} \geq 4$)
- $Q_* \sim 1$: Equipartition case
- $Q_* \ll 1$: Magnetically subdominant or kinetically dominant turbulence ($E_{\mathrm{K}} \propto k^{\alpha_{\mathrm{K}}}$, $\alpha_{\mathrm{K}} \geq 2$)

Spectral parameters

Parameters α_i, β_i, q_i, p_i

$$E_i(k,t) \propto k^{\alpha_i}$$

$$E_i(k,t) = \xi_i^{-\beta_i} \phi_i\left(k\xi_i\right)$$

$$\xi_i(t) \propto t^{q_i}$$

$$\mathcal{E}_i(t) \propto t^{-p_i}$$

pq diagram

Since $\mathcal{E}_i = \int E_i dk$, we have the relation

$$p_i = (1+\beta_i)q_i$$

Straight lines for constant β

Inverse cascade condition

$$s_i = \frac{\partial \ln E_i}{\partial \ln t} = (\alpha_i - \beta_i)\, q_i > 0$$

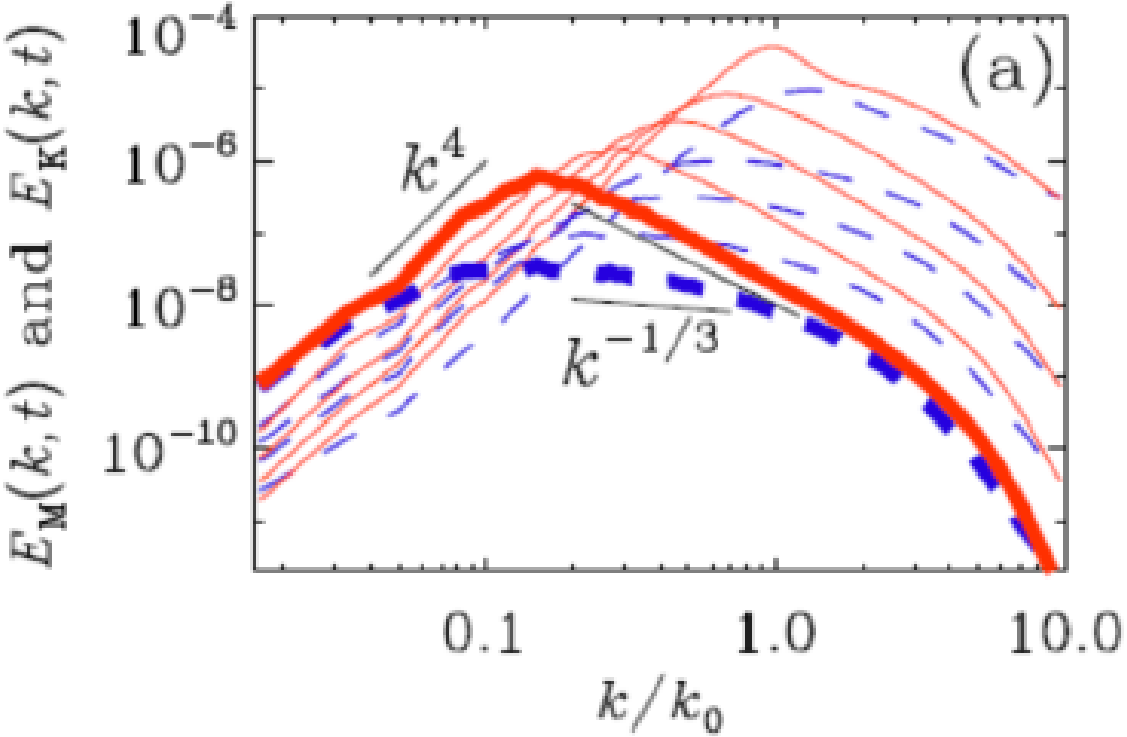

Numerical simulations

Case 1. Initial non–helical ($\sigma_{\rm M} = 0$) Batchelor spectrum ($\alpha_i = 4$)

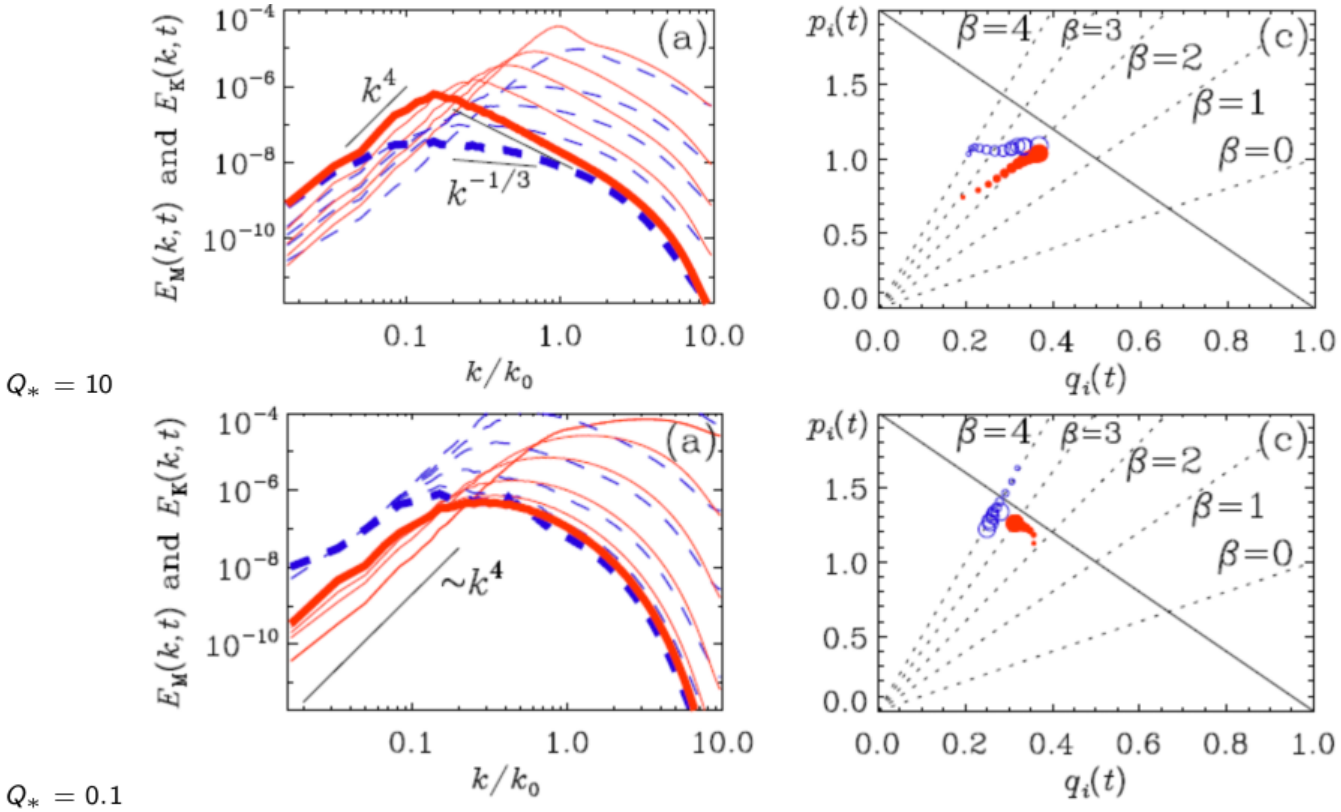

[34] A. Brandenburg, *et al. Phys. Rev. D* **96**, 123528 (2017)

Numerical simulations

Case 2. Initial helical ($\sigma_{\rm M} = 0.3$) white noise spectrum ($\alpha_i = 2$)

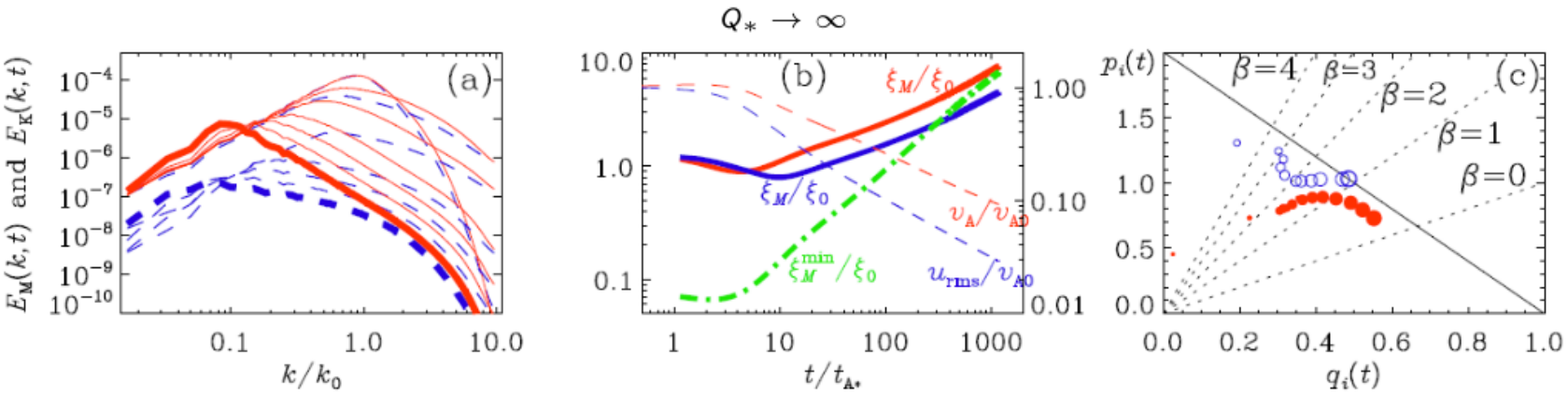

Realizability condition:

$$\frac{1}{2}k|H_{\rm M} \leq E_M \Rightarrow \xi_{\rm M} \geq \frac{\mathcal{H}_{\rm M}}{2\mathcal{E}_{\rm M}} = \xi_{\rm M}^{\rm min}$$

Numerical simulations

Case 3. Initial fully helical ($\sigma_{\mathrm{K}} = 0$) Batchelor kinetic spectrum ($\alpha_{\mathrm{K}} = 4$)

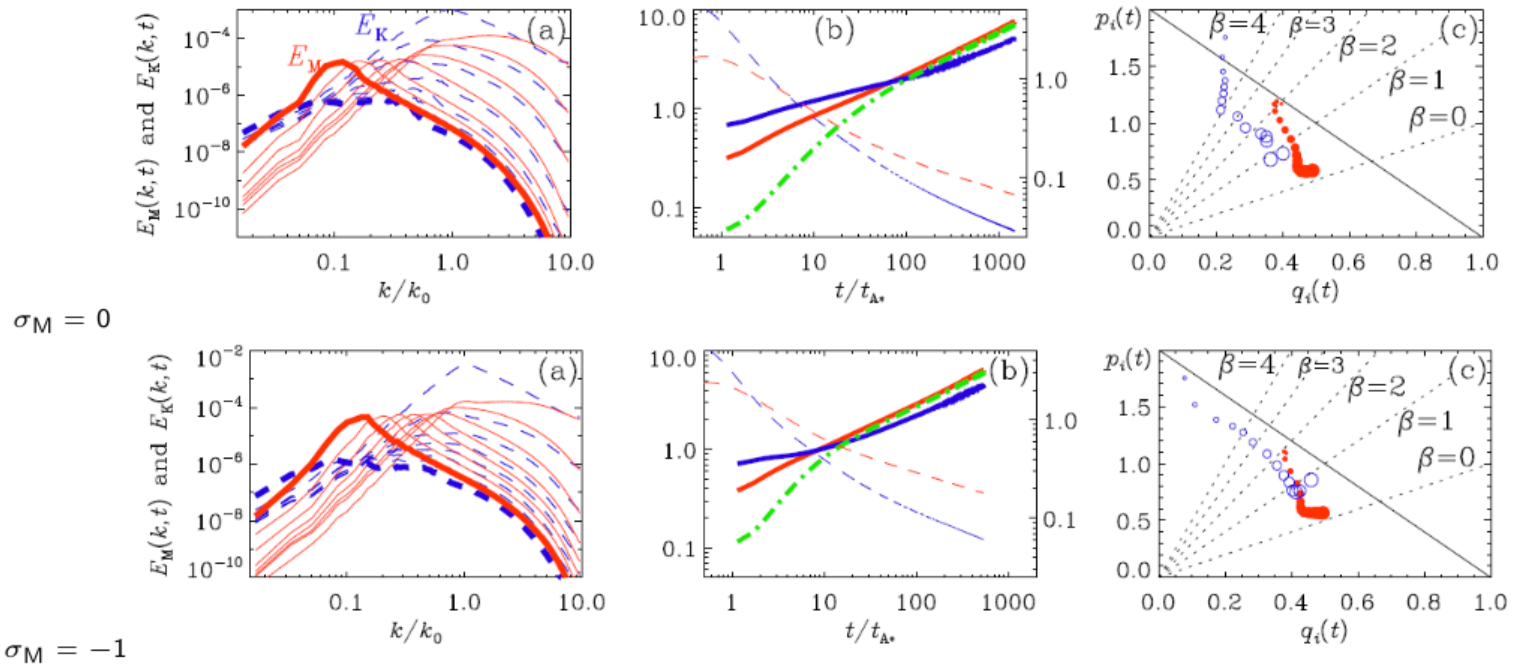

Numerical simulations

Conclusions

- Inverse cascade can be predicted with the condition $s_i = (\alpha_i - \beta_i)\, q_i > 0$
- With initial helicity, conservation of total helicity dominates ($\beta = 0$)
- With no initial helicity, pq diagram tends to $\beta = 2$ and conservation of Saffman integral dominates
- With inetically dominated turbulence, pq diagram tends to $\beta = 4$ and conservation of Loitsiansky integral dominates

- Total helicity

$$\langle \boldsymbol{\omega} \cdot \boldsymbol{u} \rangle + \langle \boldsymbol{J} \cdot \boldsymbol{B} \rangle$$

- Saffman integral

$$\mathcal{S} = \int \langle \boldsymbol{u}(\boldsymbol{x}, t) \cdot \boldsymbol{u}(\boldsymbol{x} + \boldsymbol{r}, t) \rangle d\boldsymbol{r}$$

- Loitsianski integral

$$\mathcal{L} = \int r^2 \langle \boldsymbol{u}(\boldsymbol{x}, t) \cdot \boldsymbol{u}(\boldsymbol{x} + \boldsymbol{r}, t) \rangle d\boldsymbol{r}$$

GW equation for a flat expanding Universe

- Assumptions: isotropic and homogeneous Universe.
- Friedmann–Lemaître–Robertson–Walker (FLRW) metric $\gamma_{ij} = a^2 \delta_{ij}$.
- Tensor-mode perturbations above the FLRW model:

$$g_{ij} = a^2 \left(\delta_{ij} + h_{ij}^{\rm phys} \right), \quad |h_{ij}^{\rm phys}| \ll |g_{ij}|$$

- GW equation is[35]

$$\left(\partial_t^2 - \frac{a''}{a} - c^2 \nabla^2 \right) h_{ij} = \frac{16\pi G}{\mathbf{a} c^2} T_{ij}^{\rm TT}$$

  - h_{ij} are rescaled $h_{ij} = a h_{ij}^{\rm phys}$.
  - Comoving spatial coordinates $\nabla = a \nabla^{\rm phys}$.
  - Conformal time $\mathrm{d}t = a \, \mathrm{d}t_c$.
  - Comoving stress-energy tensor components $T_{ij} = a^4 T_{ij}^{\rm phys}$.
  - Radiation-dominated epoch such that $a'' = 0$.

[35] L. P. Grishchuk, *Sov. Phys. JETP* **40**, 409 (1974).
ARP *et al.*, *Geophys. Astrophys. Fluid Dyn.* **114**, 130 (2020).

Numerical results for decaying MHD turbulence[36]

$$1152^3, k_* = 2\pi \times 100, \Omega_{\rm M} \sim 10^{-2}, \sigma_{\rm M} = 1$$

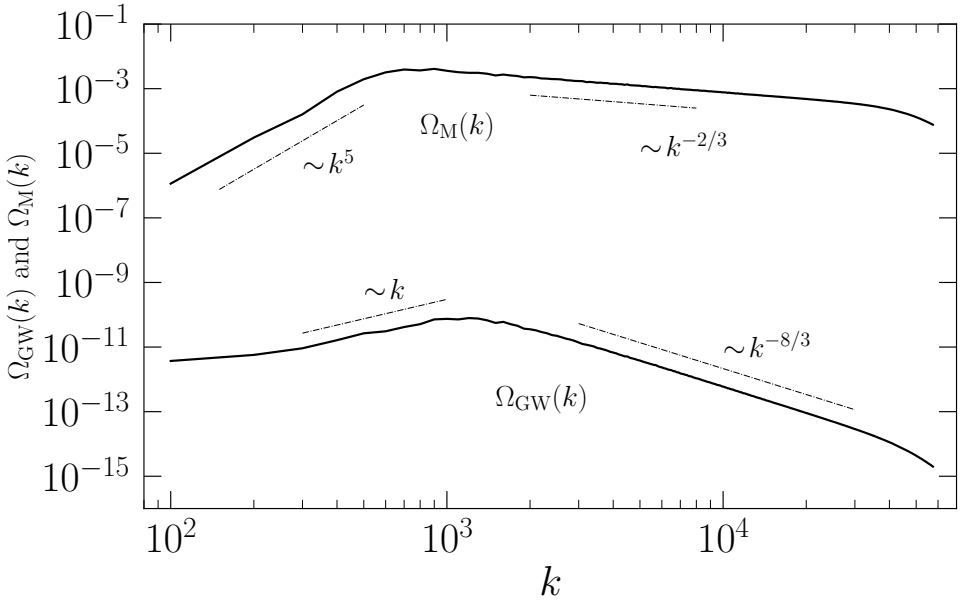

- **Characteristic k scaling in the subinertial range for the GW spectrum.**
- k^2 expected at scales $k < k_*$ and k^3 at $k < H_*$ according to the "top-hat" model (Caprini *et al.*, 2020).

[36] ARP *et al.*, *Phys. Rev. D* **102**, 083512 (2020).

Using PTA to constrain primordial magnetic fields at the QCD scale[37]

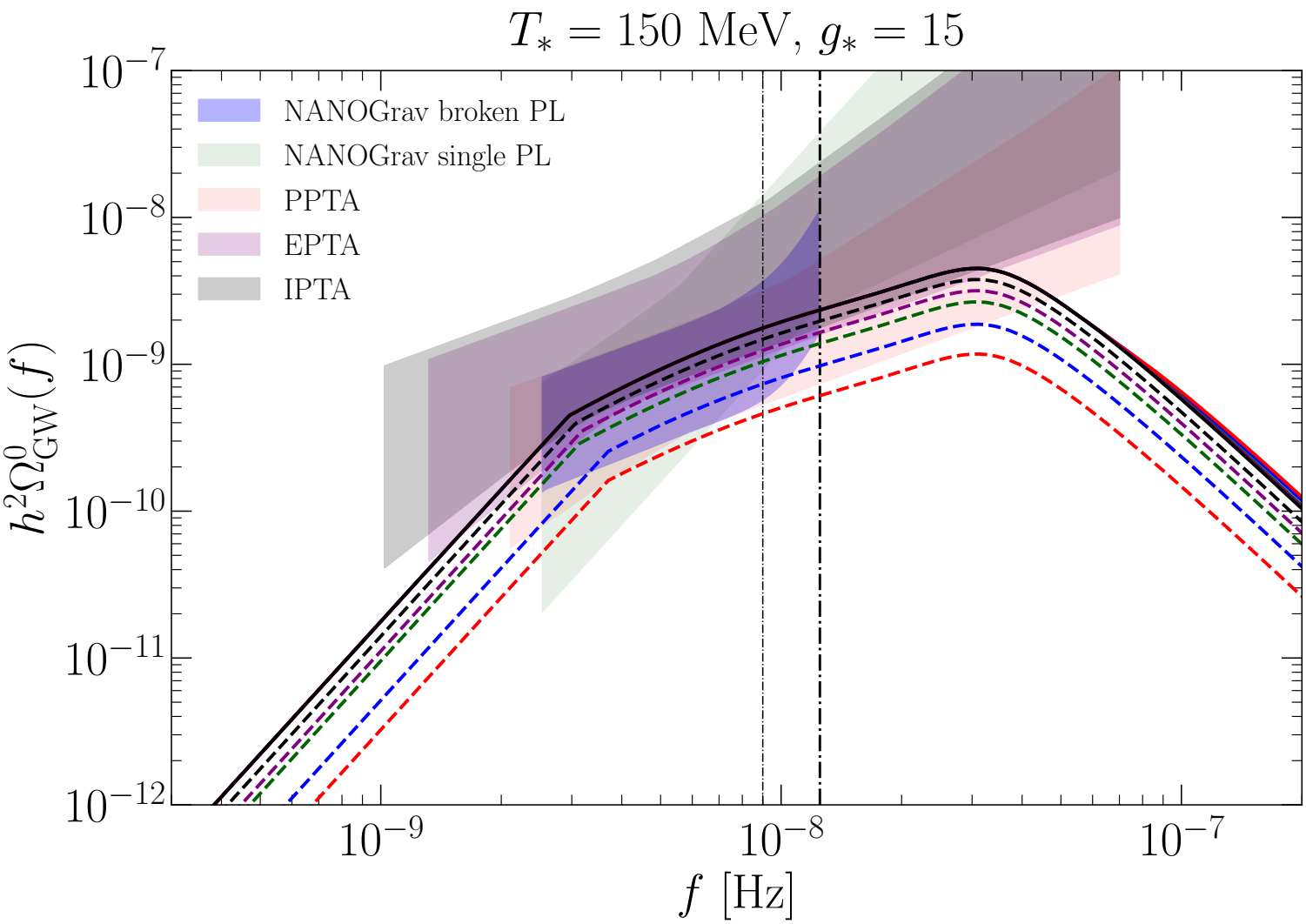

[37] ARP *et al.*, *Phys. Rev. D* **105**, 123502 (2022).

Using PTA to constrain primordial magnetic fields[38]

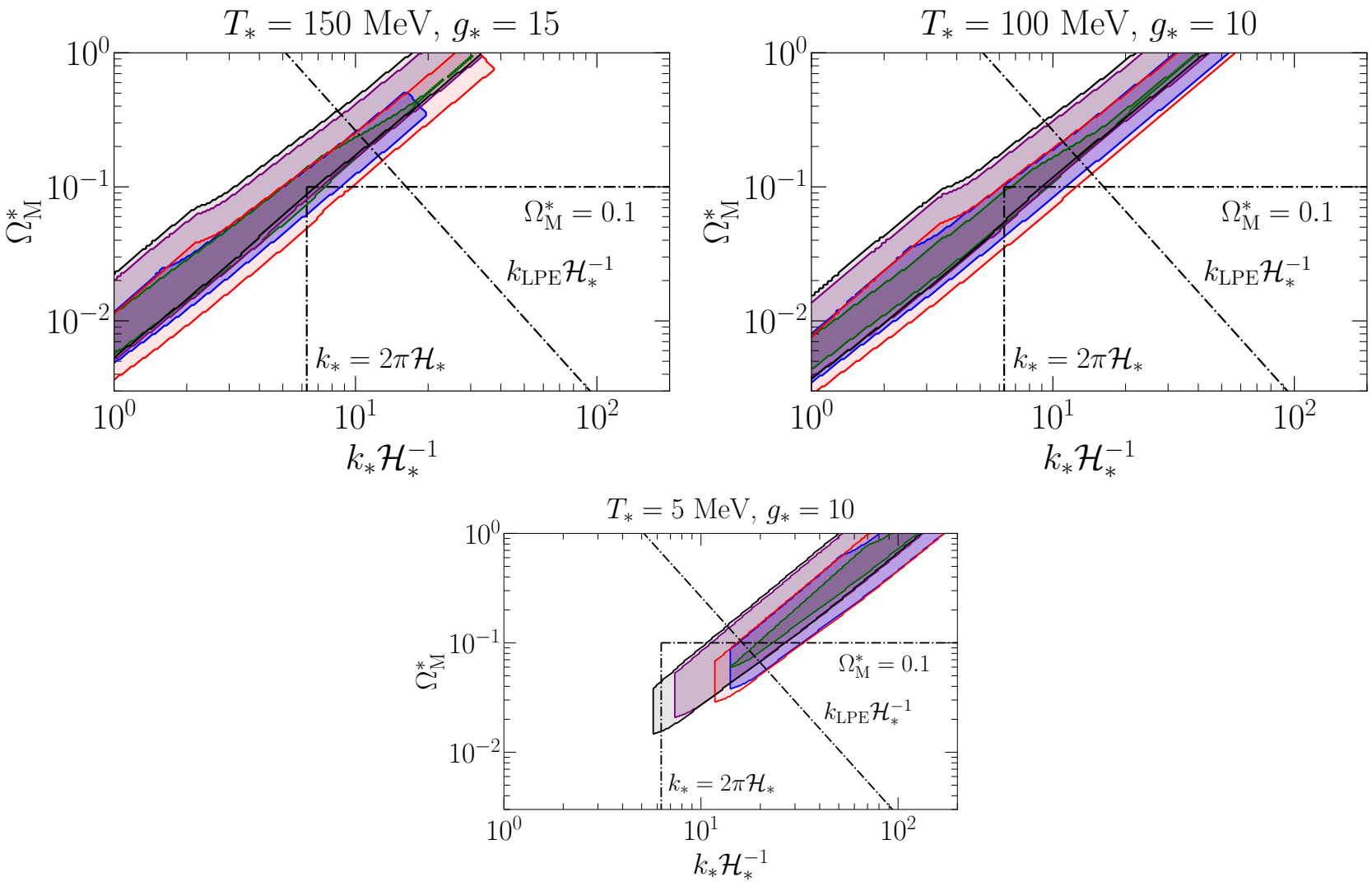

[38] ARP *et al.*, *Phys. Rev. D* **105**, 123502 (2022).

Primordial magnetic fields constraints with PTA[39]

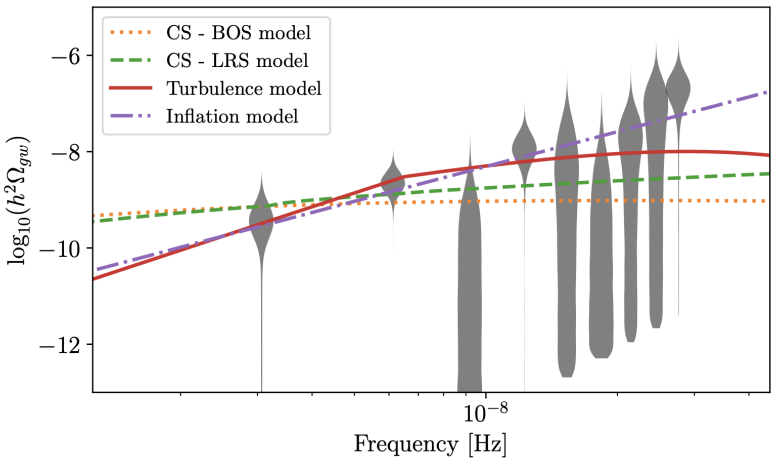

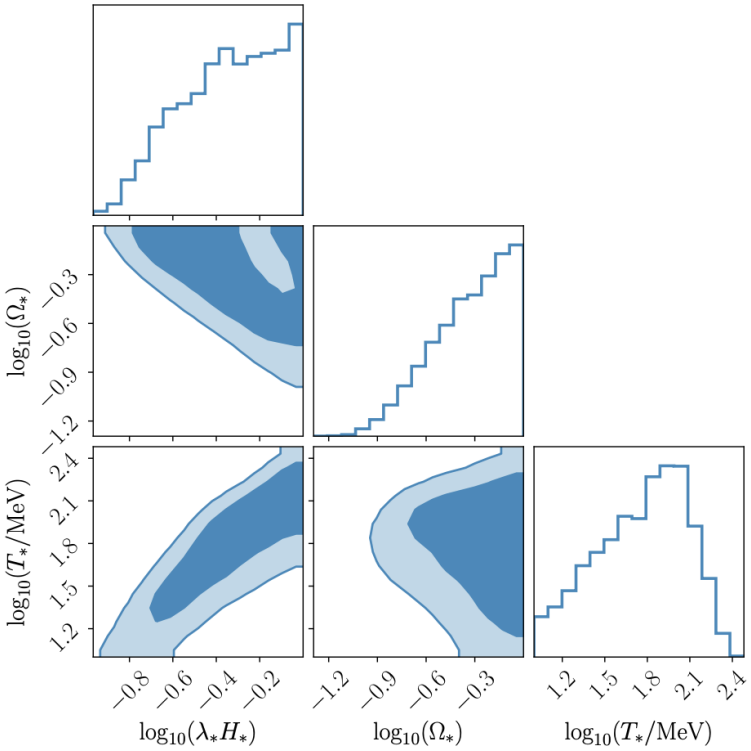

[39] [EPTA collab.] (incl. ARP), arXiv:2306.16227 (2023).

First-order phase transition parameters with LISA for sound waves + turbulence[40]

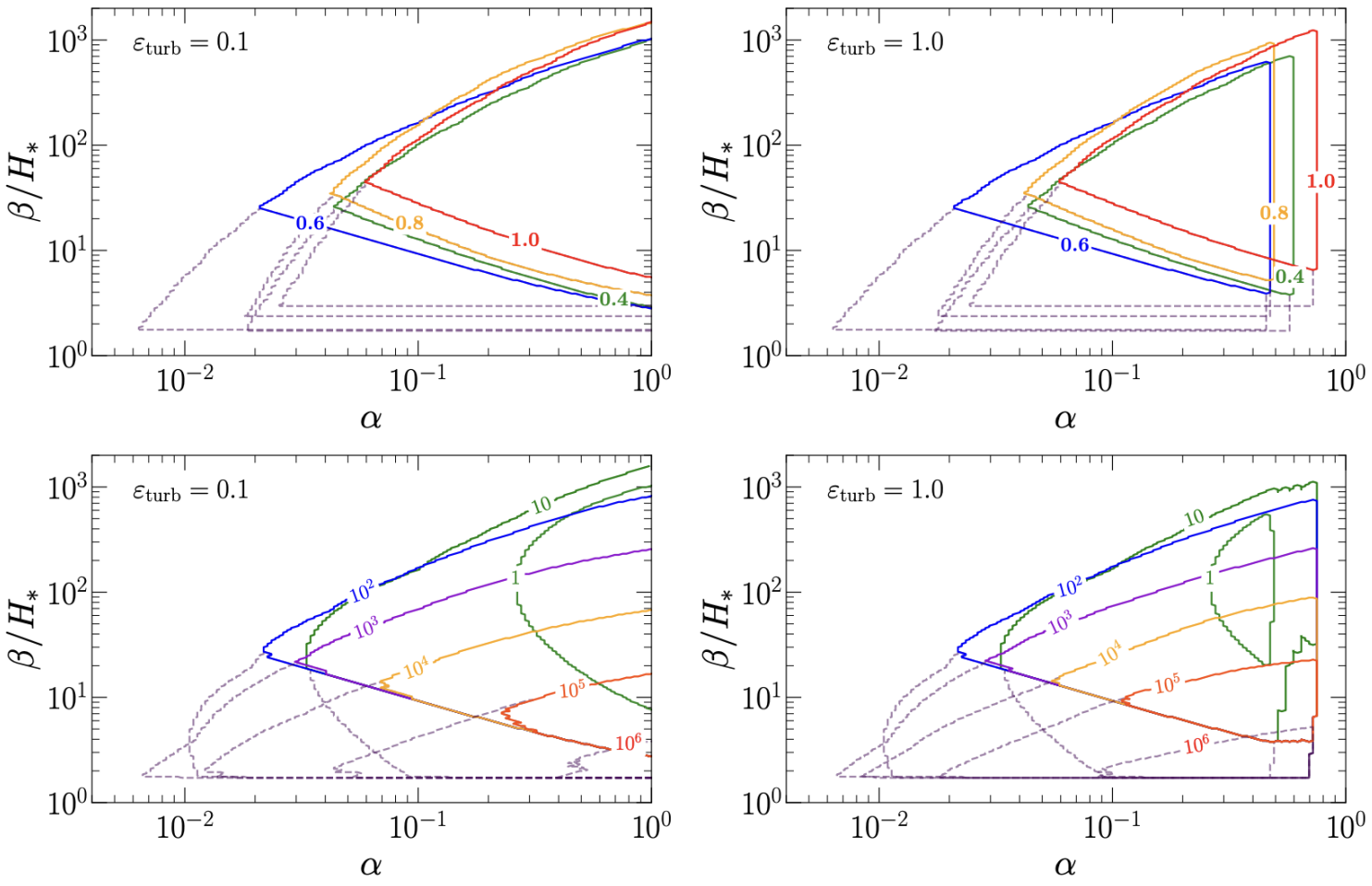

[40] ARP *et al.*, arXiv:2307.10744 (2023).

Using PTA,[41] LISA, and ET to constrain primordial magnetic fields **[unpublished]**

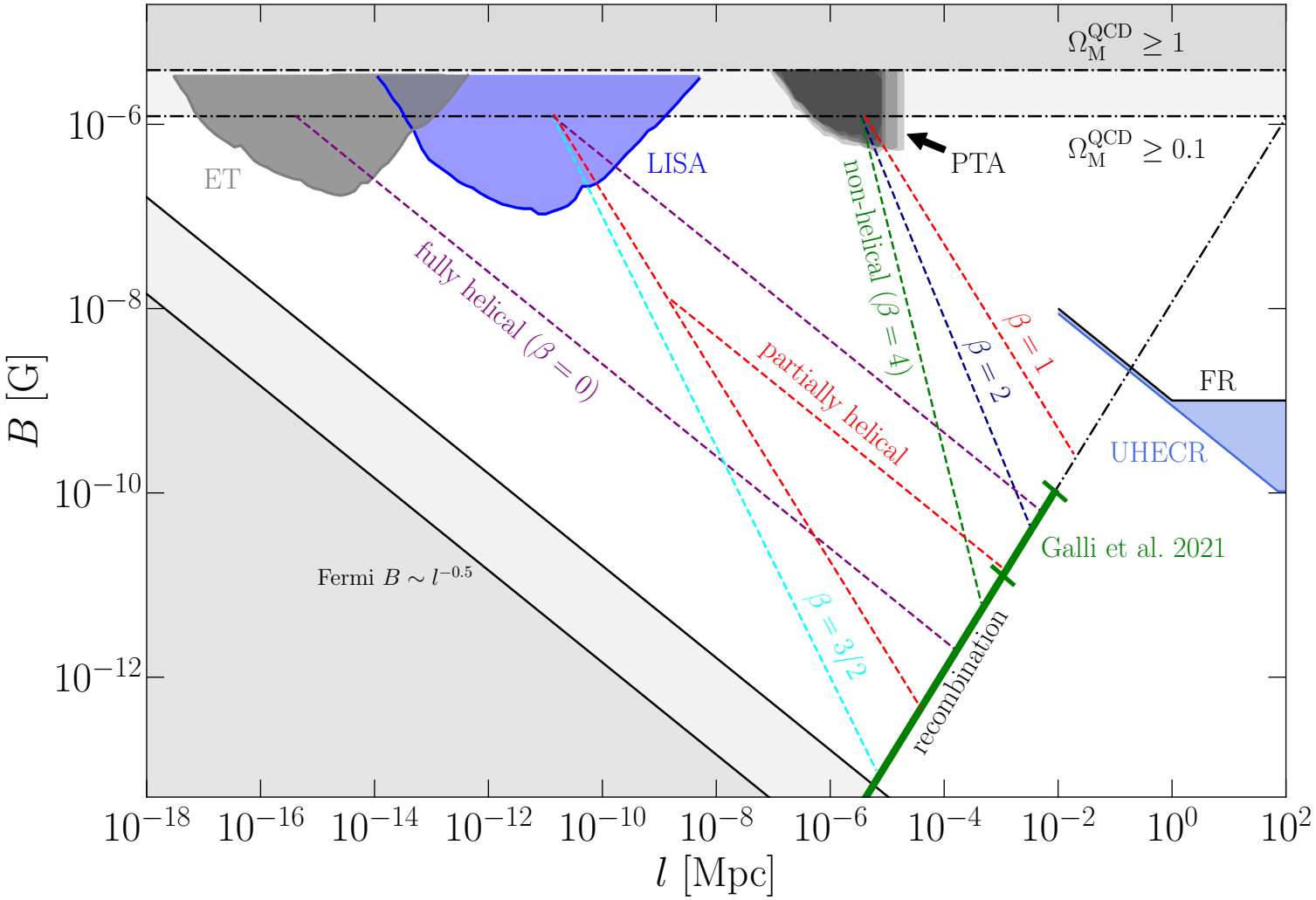

[41] ARP *et al.*, *Phys. Rev. D* **105**, 123502 (2022).

Using LISA to detect primordial magnetic fields at the EWPT scale (decaying MHD turbulence)[42]

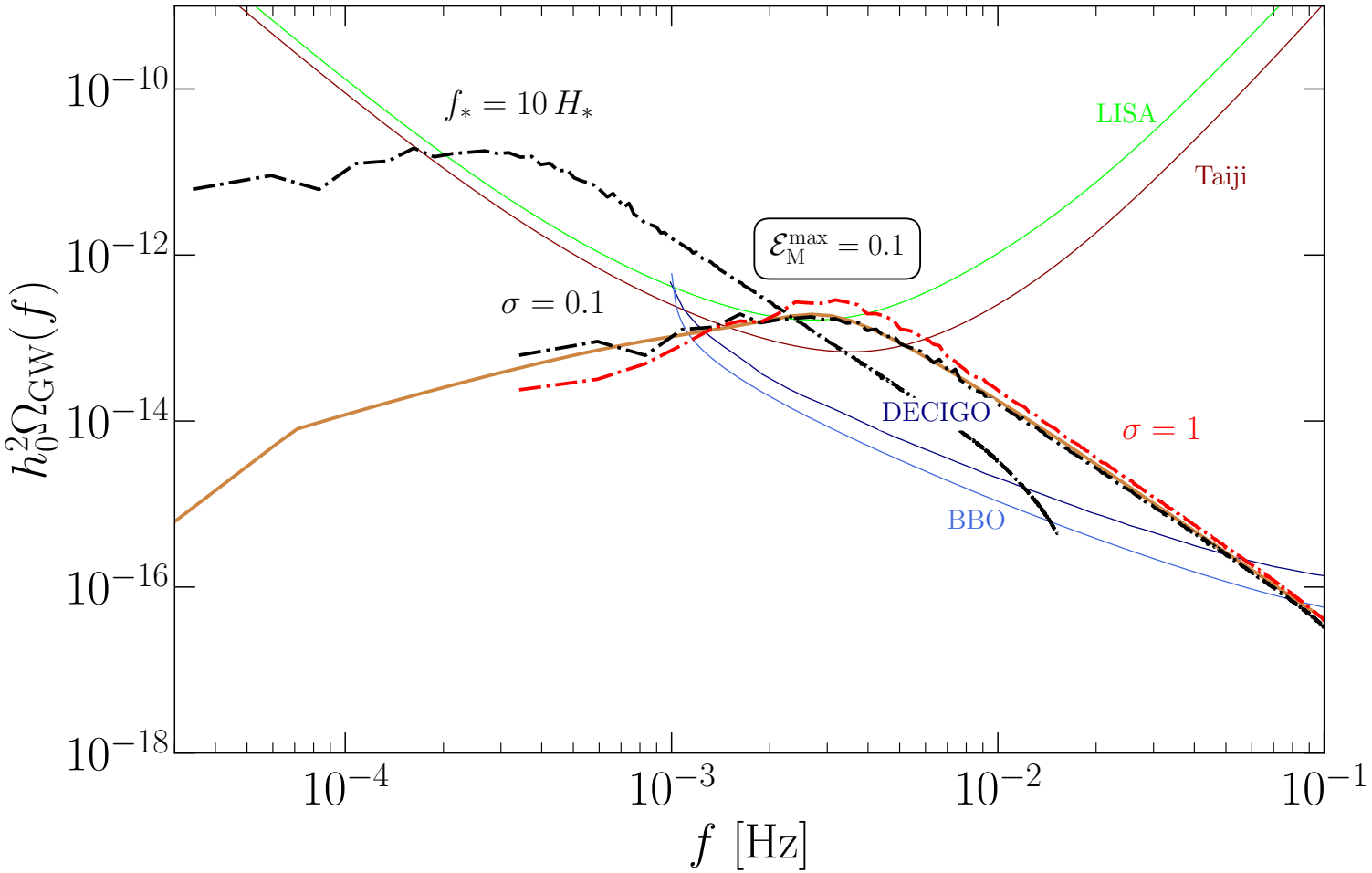

[42] ARP *et al.*, *Phys. Rev. D* **102**, 083512 (2020).
ARP *et al.*, *JCAP* **04** (2022), 019.
ARP *et al.*, *Phys. Rev. D* **105**, 123502 (2022).

Using LISA to detect primordial helical magnetic fields at the EWPT scale (decaying MHD turbulence)[43]

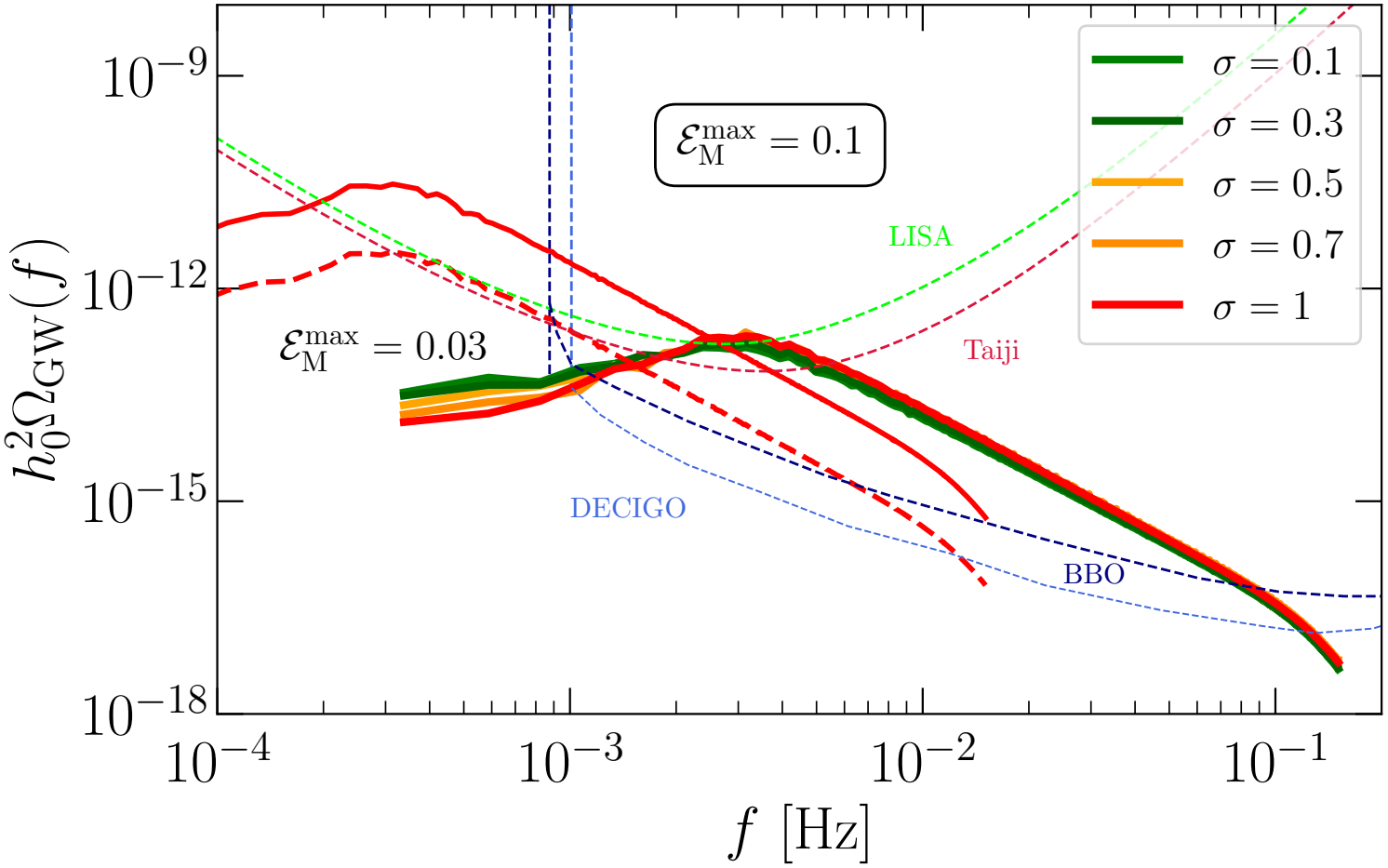

[43] ARP *et al.*, *JCAP* **04** (2022), 019.

Using LISA to detect primordial helical magnetic fields at the EWPT scale (forcing MHD turbulence)[44]

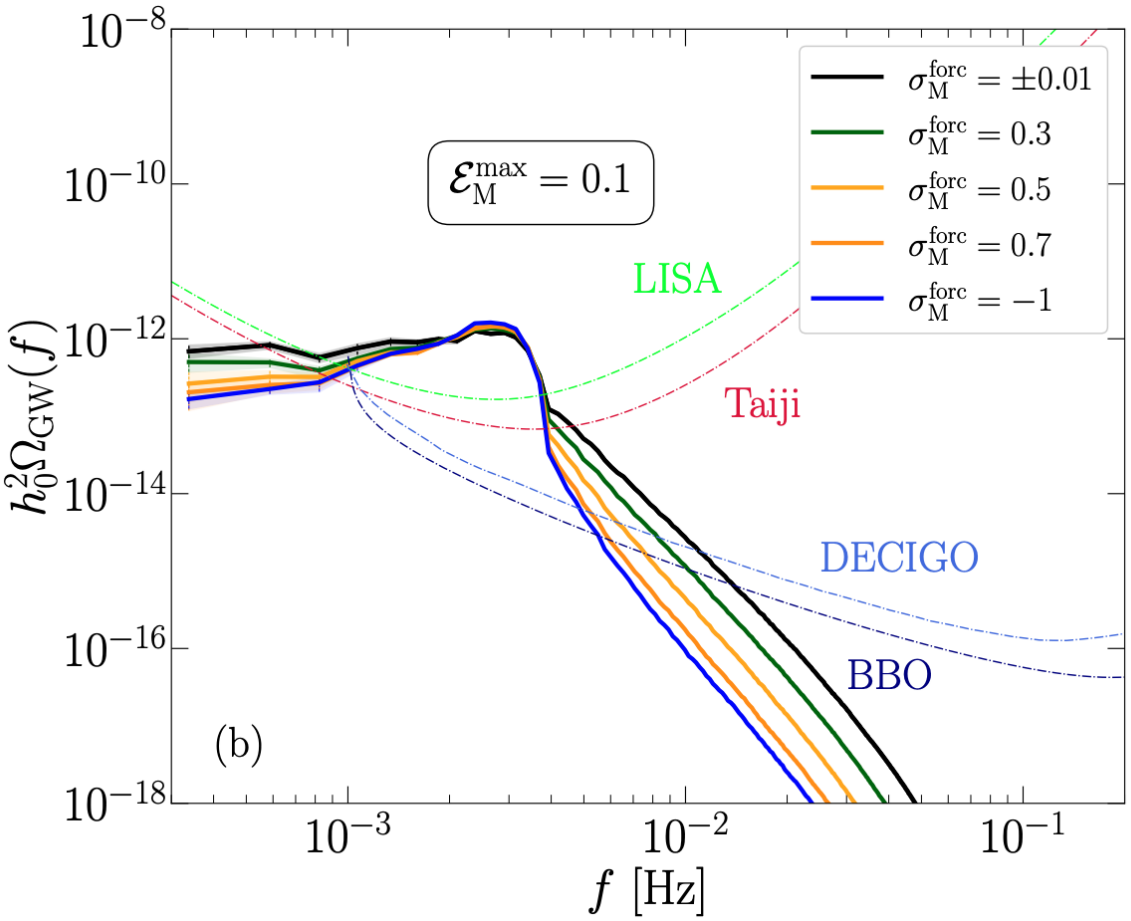

[44] ARP *et al.*, *JCAP* **04** (2022), 019.

Polarization degree from decaying turbulence (initially given field)[45]

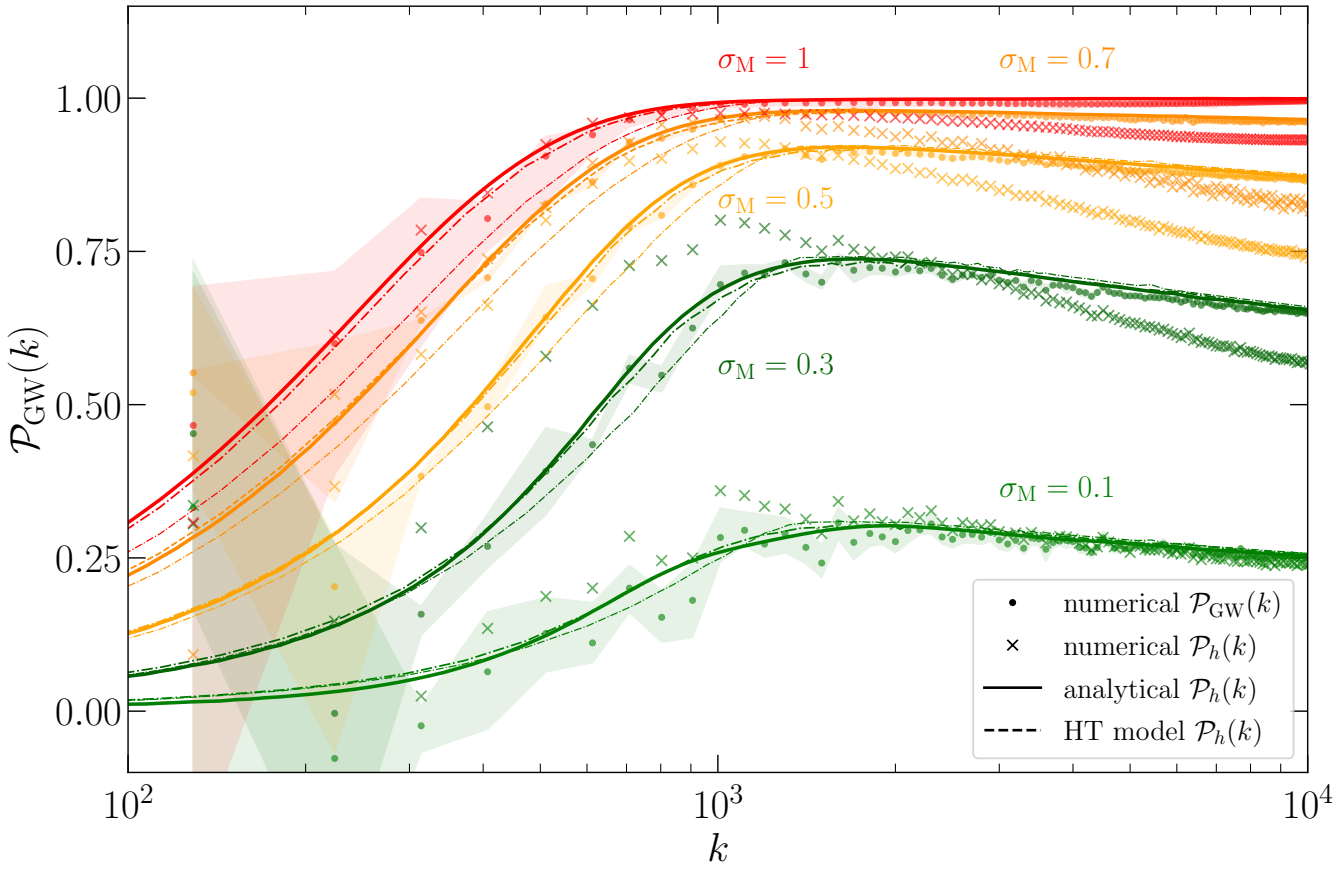

[45] ARP *et al.*, *JCAP* **04** (2022), 019.
T. Kahniashvili, G. Gogoberidze, B. Ratra, *Phys. Rev. Lett.* **95**, 151301 (2005).
L. Kisslinger, T. Kahniashvili, *Phys. Rev. D* **92**, 043006 (2015).
J. Ellis *et al.*, *JCAP* **10** (2020), 032.

Polarization degree from decaying turbulence (initially driven field)[46]

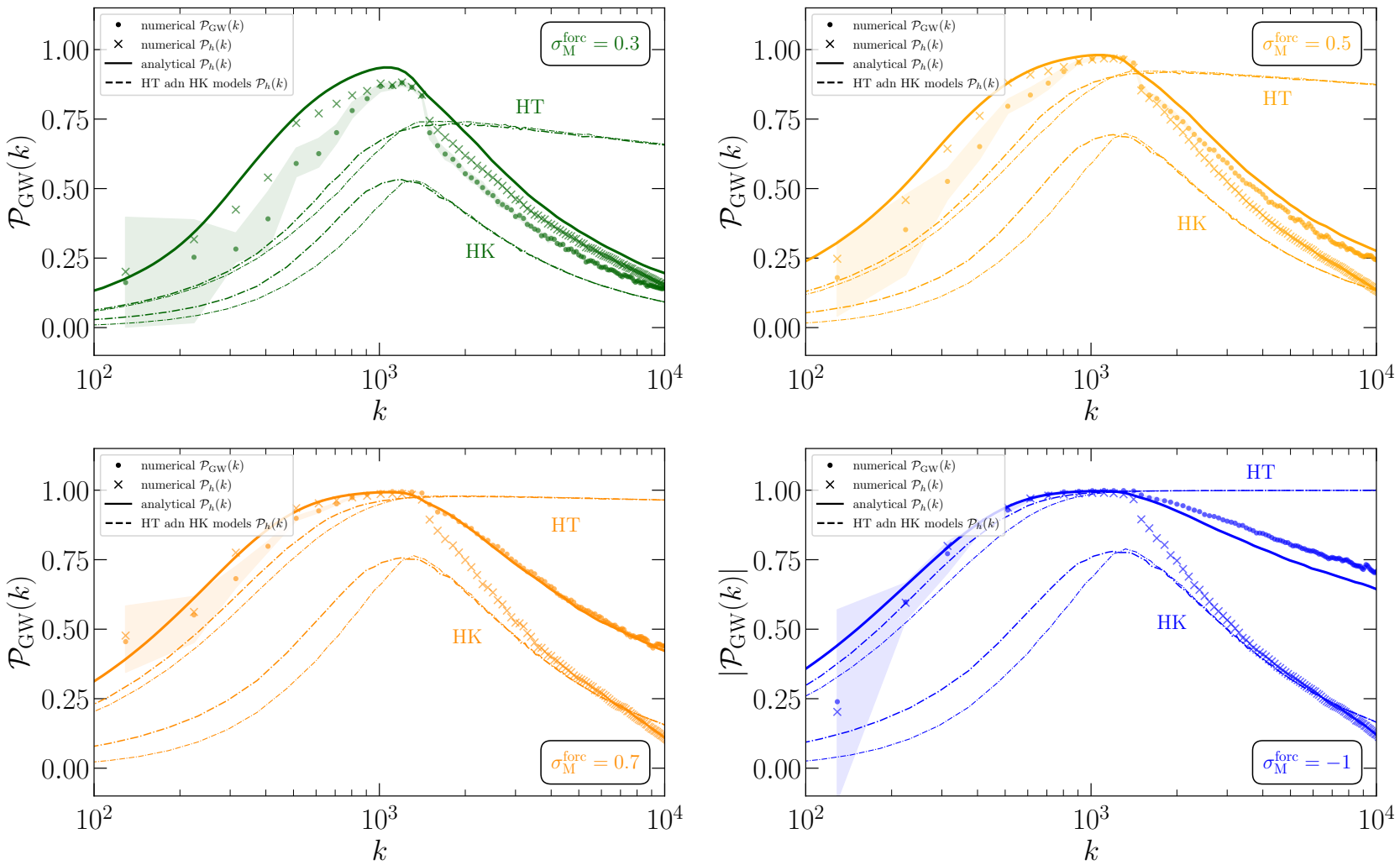

[46] ARP *et al.*, *JCAP* **04** (2022), 019.

Extended pumping of energy

- The GW energy density becomes 'stationary' after the source energy density reaches its maximum in a time scale $\delta t = t - t_* \sim 1/k_*$.
- If we extend the pumping of energy, the difference is small (~ 4 times for $\tau = 2$, $\tau > 0.5$ is highly unrealistic).[47]

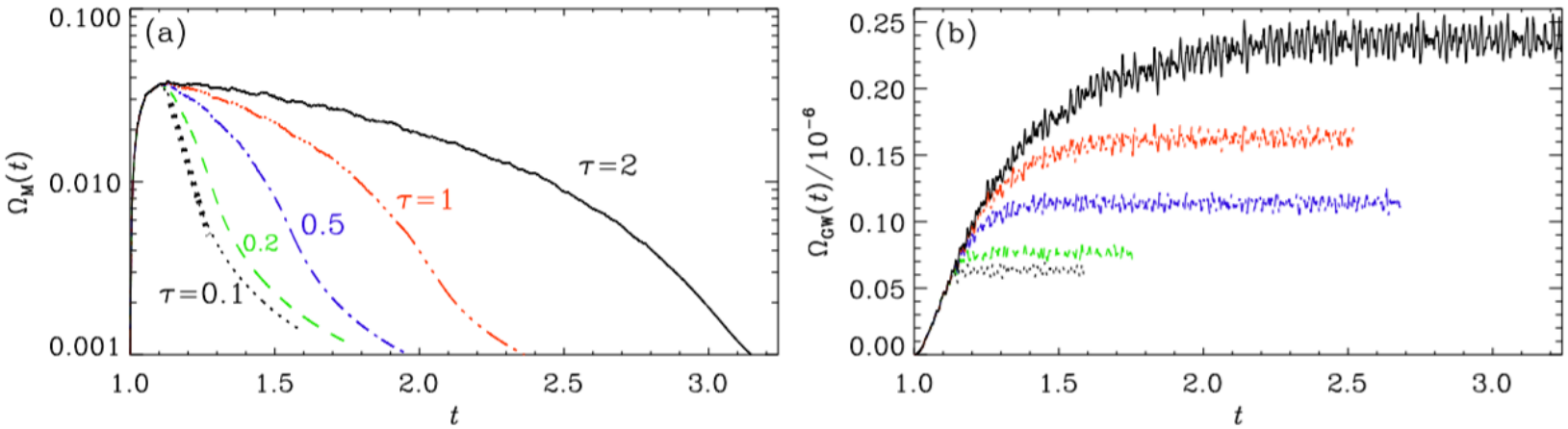

[47] T. Kahniashvili *et al.* (incl. ARP), *Phys. Rev. Res.* **3**, 013193 (2021).

Efficiency of GW production[48]

- The GW energy density is proportional to $\Omega_{\rm M}^2$ and k_*^{-2}, so one can define an efficiency factor:

$$q = \frac{k_* \Omega_{\rm GW}^{1/2}}{\Omega_{\rm M}}$$

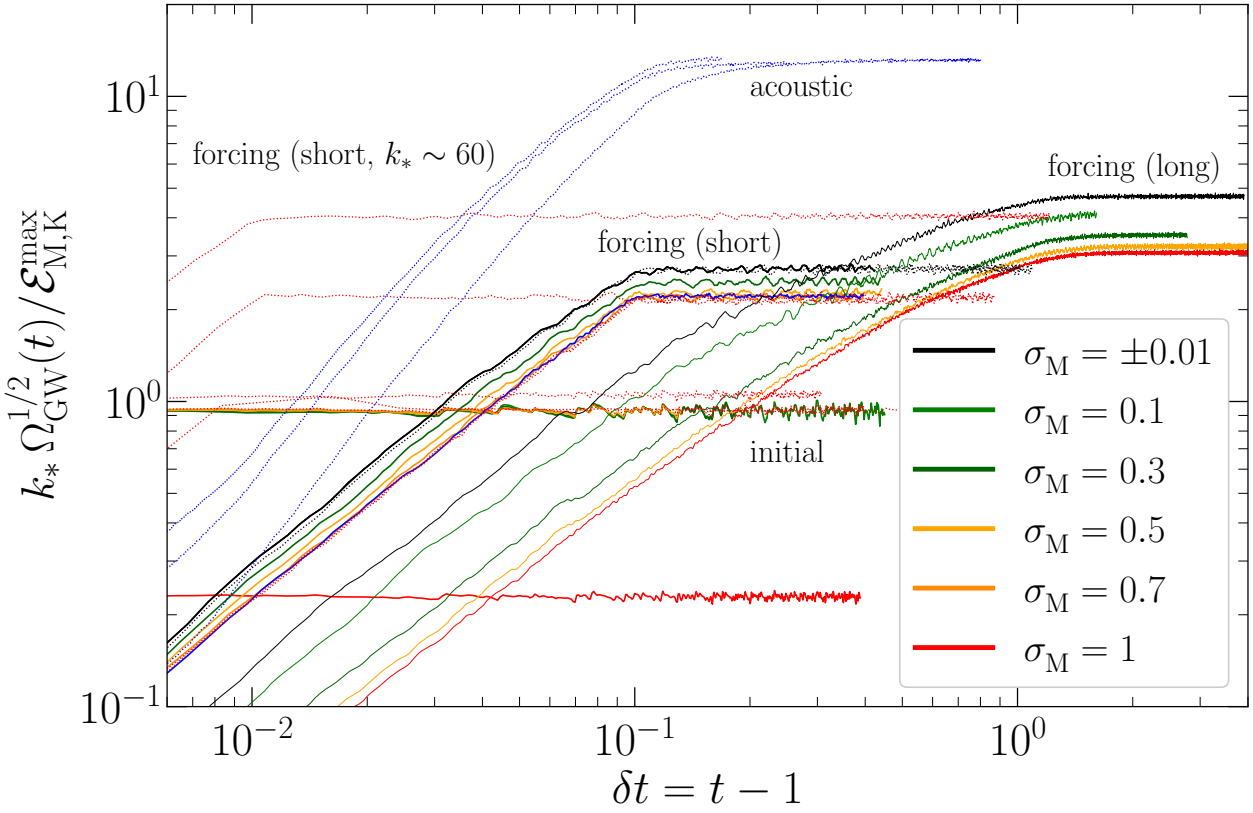

[48] ARP *et al.*, *JCAP* **04** (2022), 019.

Helicity

- Magnetic helicity is observed in present astrophysical objects.
- Fractional magnetic helicity is preferred to explain IGMF from cosmological seed fields.
- Primordial helical magnetic fields require a parity-odd violation (can be used as a test for baryogenesis, axions, ...).
- Helicity affects the dynamical evolution of the primordial magnetic fields.
- **Helical fields produce circularly polarized GWs.**

Definition (Magnetic Helicity)

$$\mathcal{H} = \left\langle \boldsymbol{B} \cdot (\boldsymbol{\nabla} \times)^{-1} \boldsymbol{B} \right\rangle = \langle \boldsymbol{A} \cdot \boldsymbol{B} \rangle$$

Using LISA and Taiji to detect the GW polarization[51]

- LISA's dipole response function can provide us with a polarized gravitational wave background due to our proper motion.[49]
- Cross-correlation of LISA and an additional space-based GW detector can improve the detectability of a polarized GW background.[50]

$$\mathcal{P}_{\rm GW}(k) = \frac{\Xi_{\rm GW}(k)}{\Omega_{\rm GW}(k)} = \frac{\left\langle \dot{\tilde{h}}_+^2 - \dot{\tilde{h}}_-^2 \right\rangle}{\left\langle \dot{\tilde{h}}_+^2 + \dot{\tilde{h}}_-^2 \right\rangle}$$

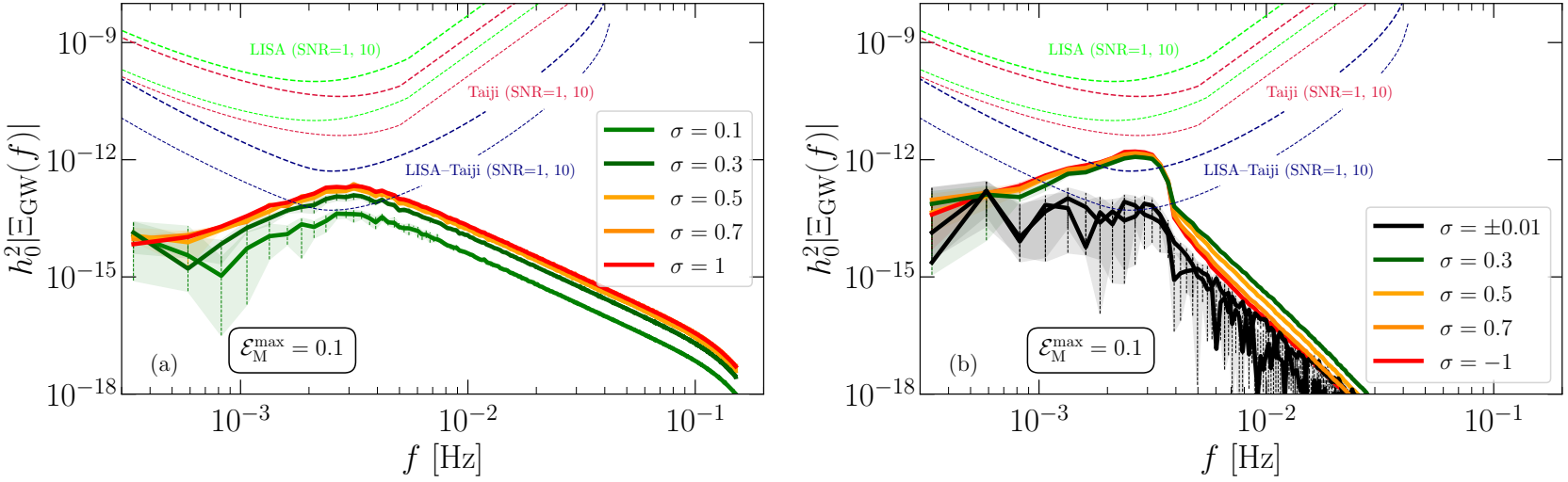

[49] V. Domcke *et al.*, *JCAP* **05** (2020), 028.
[50] G. Orlando, M. Pieroni and A. Ricciardone, *JCAP* **03** (2021), 069.
[51] ARP *et al.*, *JCAP* **04** (2022), 019.

Numerical results for forced MHD turbulence[52]

Driven magnetic (or velocity) field

- Initial magnetic and velocity fields are zero.
- The magnetic field is forced during a short duration (e.g., $0.1H_*^{-1}$) via the induction equation:

$$\frac{\partial \boldsymbol{B}}{\partial t} = \boldsymbol{\nabla} \times (\boldsymbol{u} \times \boldsymbol{B} - \eta \boldsymbol{J} + \mathcal{F}) \,.$$

- The forcing term is quasi-monochromatic with fractional magnetic helicity σ.

$$\mathcal{F} = \mathrm{Re}(\mathcal{A}\boldsymbol{f}) \exp\left[i\boldsymbol{k} \cdot \boldsymbol{x} + i\phi\right], \quad k_* - \tfrac{1}{2}\delta k \leq |\boldsymbol{k}| \leq k_* + \tfrac{1}{2}\delta k,$$

$$f_i = \left(\delta_{ij} - i\sigma\varepsilon_{ijl}\hat{k}_l\right) f_j^{(0)} / \sqrt{1+\sigma^2}.$$

[52] ARP *et al.*, *Phys. Rev. D* **102**, 083512 (2020).
ARP *et al.*, *JCAP* **04** (2022), 019.

Forcing terms

Acoustic forcing[53] on velocity fields:

- Forcing from Gaussian potential

$$\boldsymbol{f} = \nabla\phi$$

$$\phi = N\exp([\boldsymbol{x} - \boldsymbol{x}_f]^2/R^2)$$

$$N = k_{\mathrm{K}}/(2\pi)$$

- Monochromatic forcing in momentum equation.

$$\nabla \times \boldsymbol{u} = 0$$

Helical forcing[54] on magnetic fields:

- Fully helical forcing term (in Fourier space)

$$\boldsymbol{f}_{\boldsymbol{k}} = \frac{\boldsymbol{k} \times (\boldsymbol{k} \times \hat{\boldsymbol{e}}) - ik(\boldsymbol{k} \times \hat{\boldsymbol{e}})}{2k^2\sqrt{1 - (\boldsymbol{k} \cdot \hat{\boldsymbol{e}})^2/k^2}}$$

- Monochromatic forcing in induction equation.

$$\nabla \cdot \boldsymbol{B} = 0$$

[32] A. J. Mee, A. Brandenburg, *Mon. Not. Roy. Astron. Soc.* **370**, 415 (2006).

[54] A. Brandenburg, *Astrophys. J.* **550**, 824 (2001).

Using LISA to detect primordial magnetic fields at the EWPT scale (forcing MHD turbulence)[55]

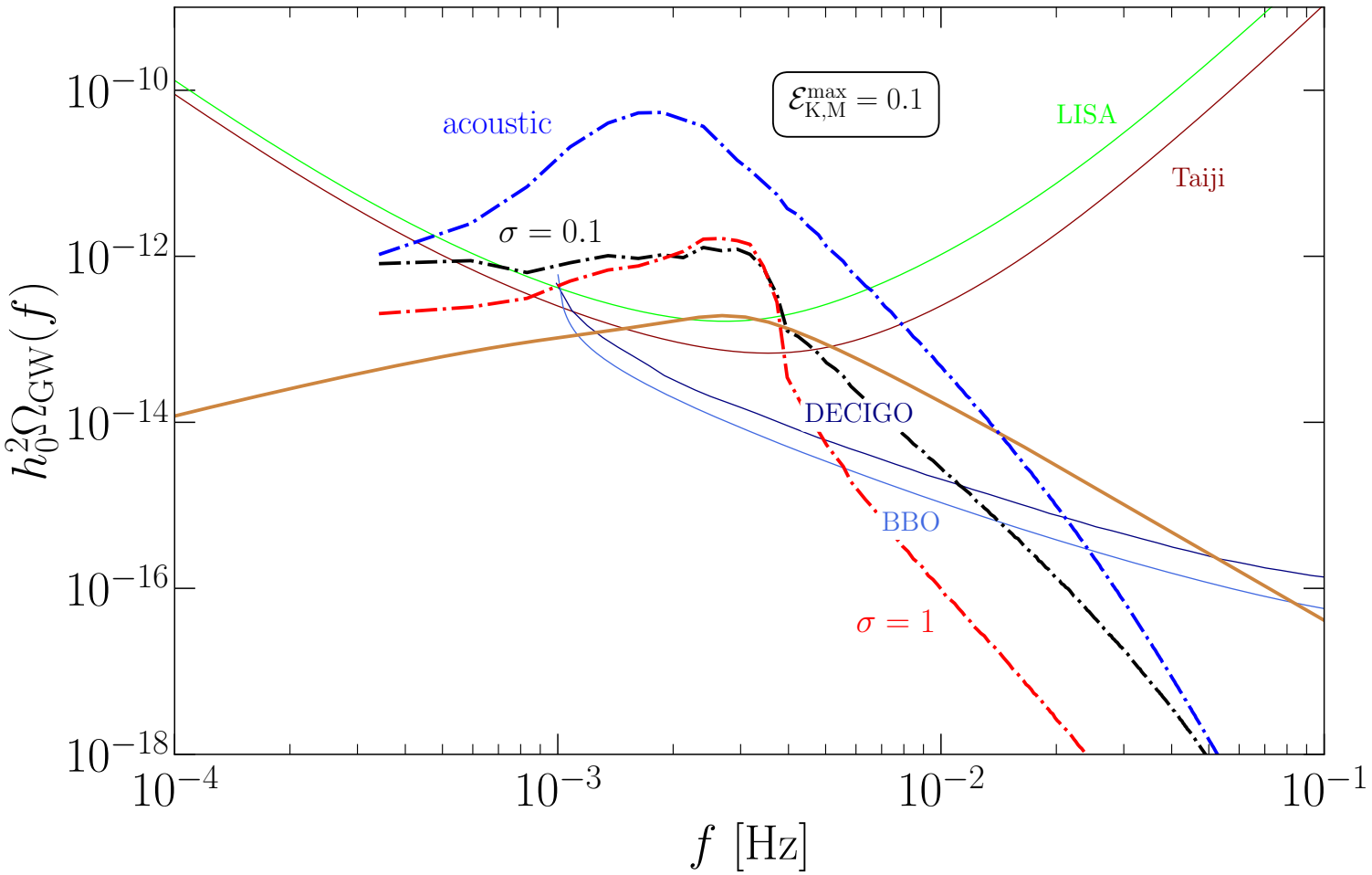

[55] ARP *et al.*, *Phys. Rev. D* **102**, 083512 (2020).
ARP *et al.*, *JCAP* **04** (2022), 019.
ARP *et al.*, *Phys. Rev. D* **105**, 123502 (2022).

LISA and LHC complementarity[56]

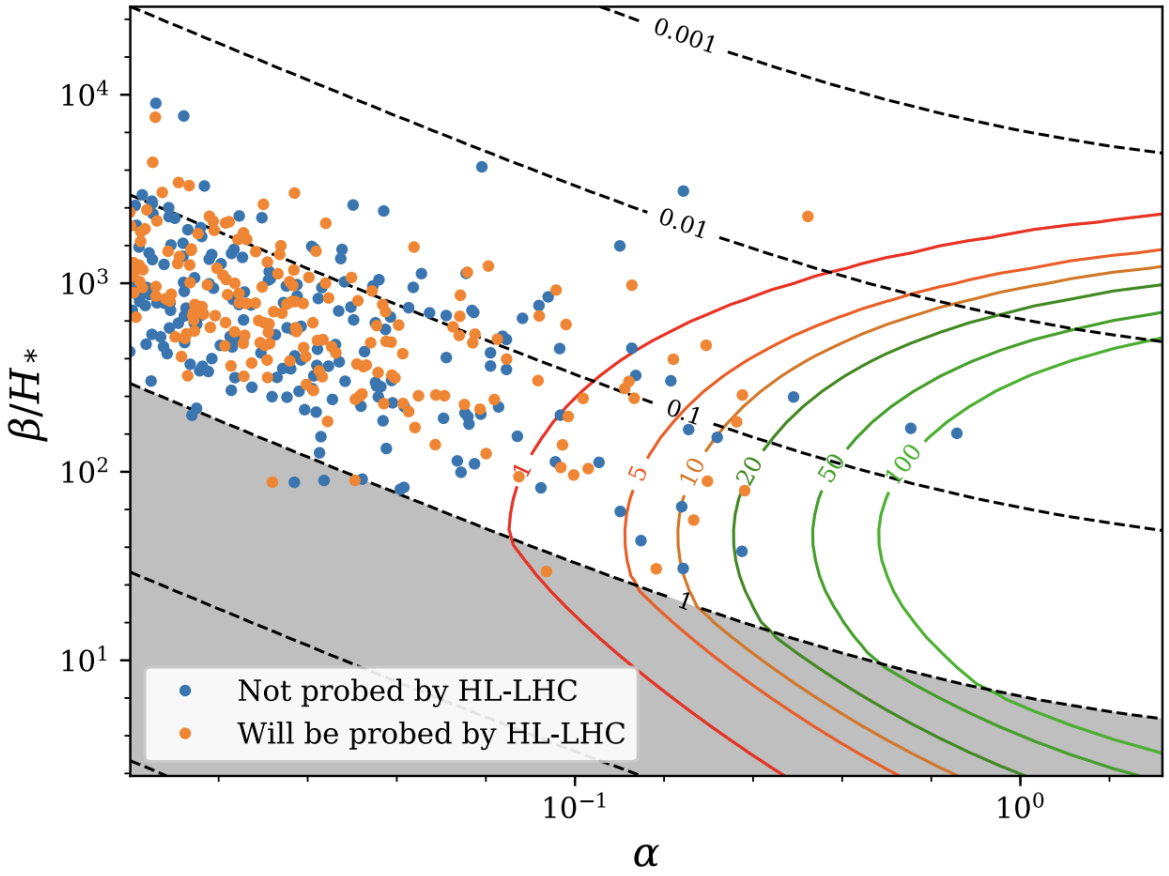

LISA sensitivity in the general singlet extension of the SM.

[56] C. Caprini *et al.*, *JCAP* **03** (2020), 024.

Comparison of decaying[57] to driven turbulence[58] and inflationary magnetogenesis with end-of-reheating T around the QCD scale[59]

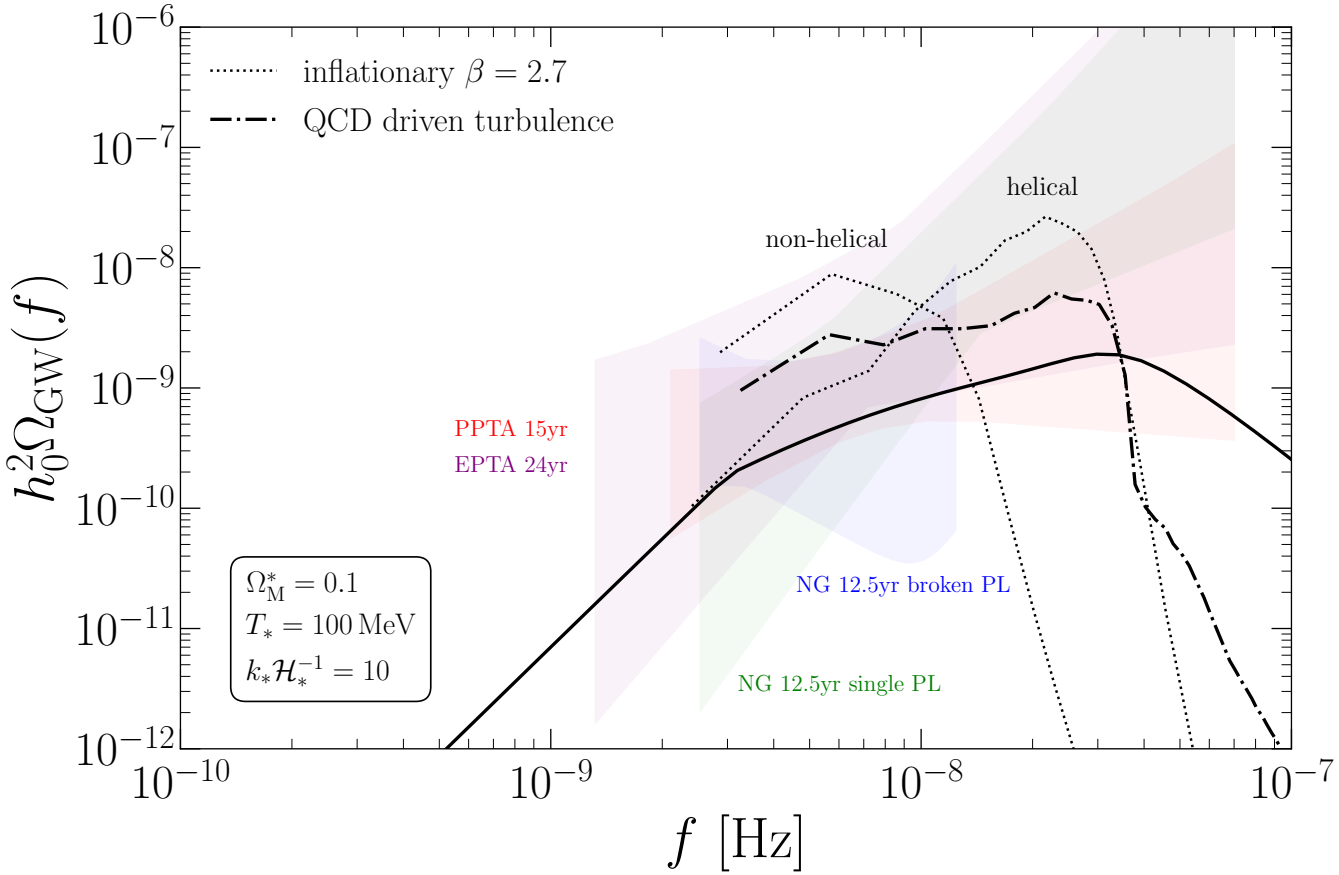

[57] ARP *et al.*, *Phys. Rev. D* **105**, 123502 (2022).

[58] E. Clarke *et al.*, *Phys. Rev. D* **104**, 043513 (2021).

[59] Y. He, ARP and A. Brandenburg, *submitted to Phys. Rev. D*, arXiv:2110.14456 (2021).

Initially given field vs forced field

- Time evolution of energy density[60]

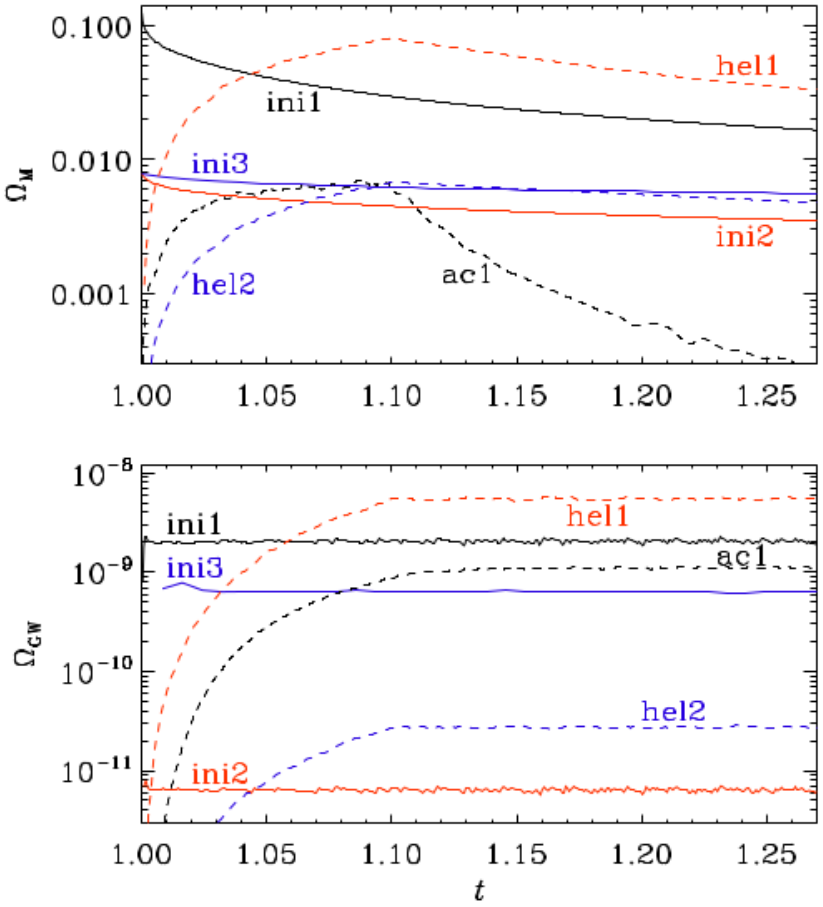

[60] ARP *et al.*, *Phys. Rev. D* **102**, 083512 (2020).

Scalar-vector-tensor (SVT) decomposition

Back to the question of efficiency (vortical vs acoustic) [61]

- GWs are sourced by the traceless-and-transverse TT projection of the stress tensor.
- SVT decomposition of $T_{ij} \to S, \sigma, \bar{\sigma}_i, \bar{\sigma}_{ij}$:

$$T_{ij} = S\delta_{ij} + \nabla_{\langle i}\nabla_{j\rangle}\sigma + \nabla_{(i}\bar{\sigma}_{j)} + \bar{\sigma}_{ij}$$

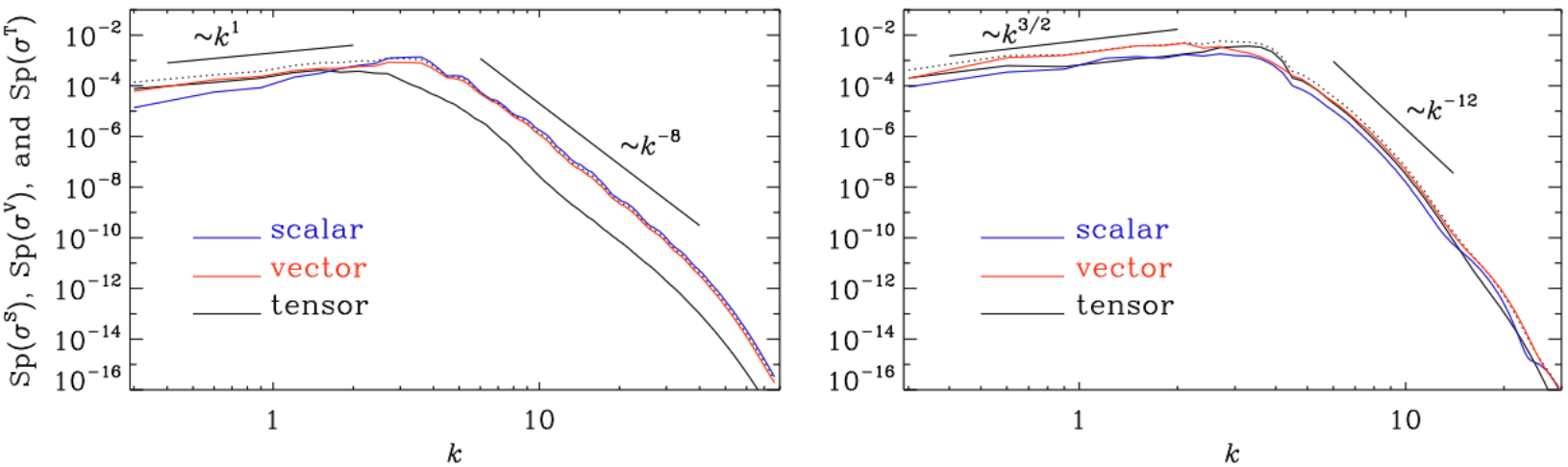

[61] A. Brandenburg, G. Gogoberidze, T. Kahniashvili, S. Mandal, ARP, N. Shenoy, *Class. Quantum Grav.* **38**, 145002 (2021), arXiv:2103.01140.

Scalar-vector-tensor (SVT) decomposition

Back to the question of efficiency (vortical vs acoustic)
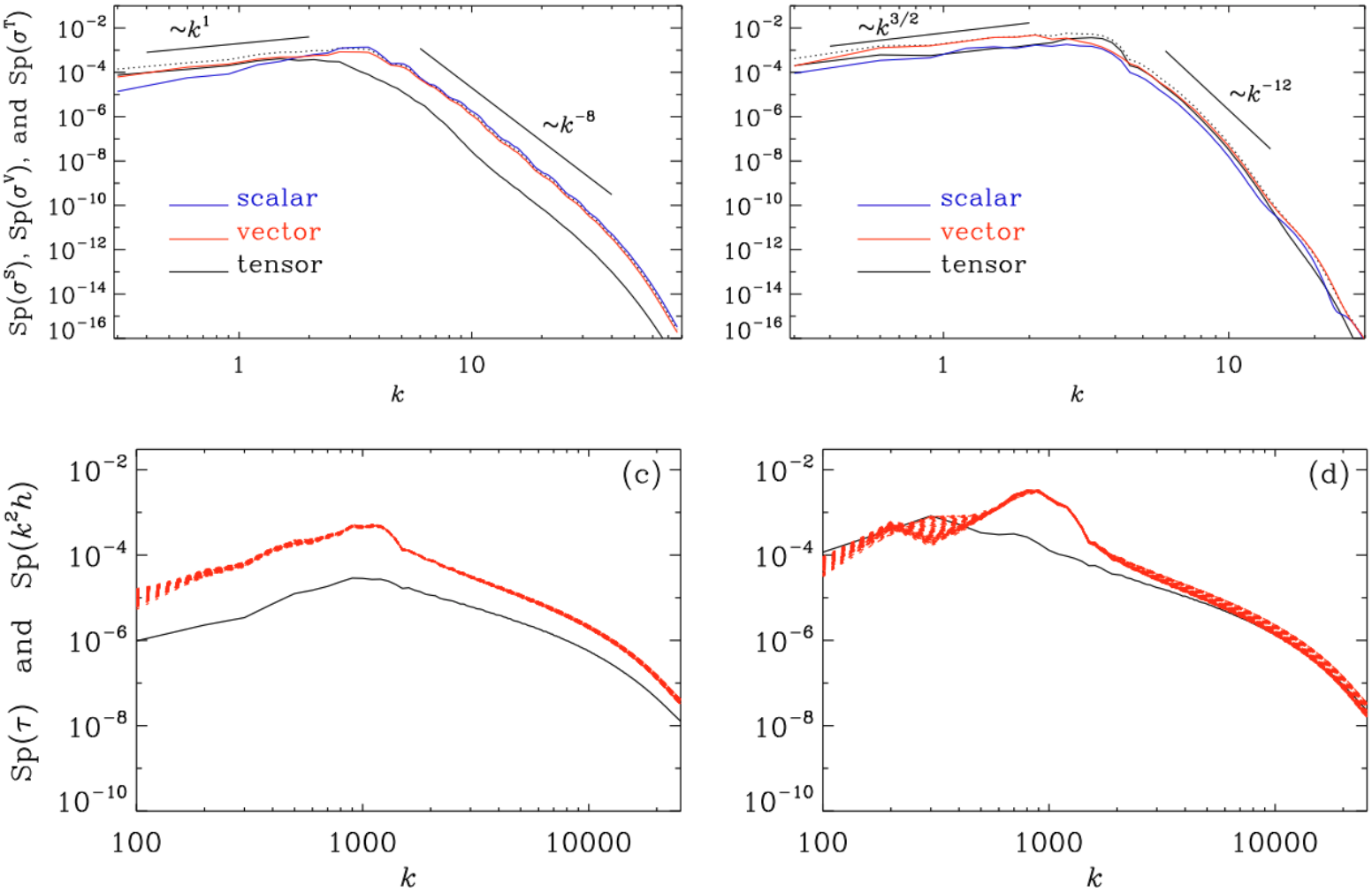
- Vortical turbulence
- Acoustic turbulence